

100 mM DTT) and heated at 100 °C for 3 min. The sample were separated by 12.5% sodium dodecyl sulfate-polyacrylamide gel electrophoresis and transferred onto polyvinylidene difluoride membranes (Immobilon-P; Millipore, Bedford, MA) by semi-dry electroblotting. The blots were blocked for 1 h at room temperature with 5% ECL advance blocking agents (GE Healthcare Bio-sciences Corp., Piscataway, NJ) in PBS containing 0.05% Tween 20 (PBS-T). The blots were washed once with PBS-T and incubated for 1 h at room temperature with a primary antibody specific for heme oxygenase-1 (heme oxygenase-1 (C-20) affinity purified goat polyclonal antibody, Santa Cruz Biotechnology, Inc., Santa Cruz, CA) in PBS-T. The blots were washed 3 times with PBS-T and incubated with the secondary antibody (horseradish peroxidase-linked anti-goat IgG (H + L) (Invitrogen, Eugene, OR)) for 1 h at room temperature. The blots were washed 3 times with PBS-T and immunoblots were visualized using an ECL system (ECL Advance Western Blotting Detection Kit; GE Healthcare Bio-sciences Corp.) with LAS-4000EPUVmini (Fujifilm, Tokyo, Japan).

#### 2.14. Measurement of liver $\text{NO}_2^-$ and $\text{NO}_3^-$ levels

$\text{NO}_2^-$  and  $\text{NO}_3^-$  ( $\text{NO}_x$ ) levels in liver homogenates were analyzed using an automated NO detector-high-performance liquid chromatographic system (ENO-10, Eicom, Kyoto, Japan) [17].

#### 2.15. Data analyses

Pharmacokinetic analyses after rHSAs administration were based on a two-compartment model. Pharmacokinetic parameters were calculated by fitting using MULTI, a normal least-squares program [18]. The uptake clearance ( $\text{CL}_{\text{uptake}}$ ) was calculated, as described in a previous report, using integration plot analysis at designated times (from 1 min to 30 min) during which the efflux and/or elimination of radioactivity from tissues were negligible [19]. Data are shown as means  $\pm$  SD for the indicated number of animals. The overall differences between groups were determined by one-way of analysis of variance (ANOVA). A probability value of  $p < 0.05$  was considered to indicate statistical significance.

### 3. Results and discussions

#### 3.1. Production of mannosylated recombinant HSAs (Man-rHSAs)

SDS-PAGE analysis clearly showed that the molecular weights of the mutants were increased slightly compared to that of wild-type rHSA, especially TM-rHSA, suggesting that multiple oligosaccharide chains were attached to TM-rHSA (Fig. 1A). To confirm that the increase in

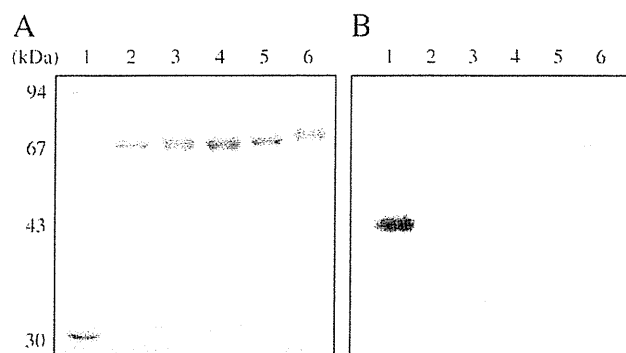


**Fig. 1.** SDS-PAGE analysis of rHSAs. A, CBB stained after SDS-PAGE. Lane 1, molecular weight marker; lane 2, wild type; lane 3, D63N; lane 4, A320T; lane 5, D494N; lane 6, TM. B, PAS stained after SDS-PAGE. Lane 1,  $\alpha_1$ -acid glycoprotein; lane 2, wild type; lane 3, D63N; lane 4, A320T; lane 5, D494N; lane 6, TM.

molecular weight of the mutants caused by newly introduced oligosaccharide chains, the periodic acid Schiff (PAS)-stain, which specifically stains oligosaccharide, was performed (Fig. 1B). In contrast to wild-type rHSA, all of the mutants reacted positively with the PAS-stain, indicating that the mutants clearly contained attached oligosaccharide chains.

The molecular weights of the rHSAs were determined to be 66537, 66849, 67097, 68977 and 69124 Da for wild-type, D63N, A320T, D494N and TM-rHSA, respectively, by MALDI-TOF-MASS analyses. To deduce how many Man residues were attached to each mutant, we took into consideration 2 GluNAc (MW: 221 Da) in determining the numbers of Man residues because N-linked oligosaccharide chains expressed in *P. pastoris* generally consist of 2 GluNAc followed by 8 to 14 Man residues [20]. As a total number of residues, D63N, A320T, D494N and TM-rHSAs would be expected to contain 1–2, 2–3, 13 and 14 of GluNAc and Man residues, respectively. These findings are in good agreement with previous data reported on the characteristics of oligosaccharide chains in other recombinant glycoproteins expressed in *P. pastoris* [20].

#### 3.2. Physicochemical properties of Man-rHSAs

To examine the effect of mutations as the result of the introduction of oligosaccharide chains on the secondary and tertiary structures of HSA, CD measurements were performed in the far- and near-UV regions (Fig. 2). All of the rHSAs showed nearly identical CD spectra in both UV regions, indicating that the mutations caused no significant effect on the secondary and tertiary structure of HSA. In addition, the effect of mutations on surface charges of rHSA was estimated by capillary electrophoresis analysis. As expected, the retention times of the Man-rHSAs were not significantly different from that of wild-type rHSA (retention time: 9.1 min for wild type; 9.0 min for D63N;

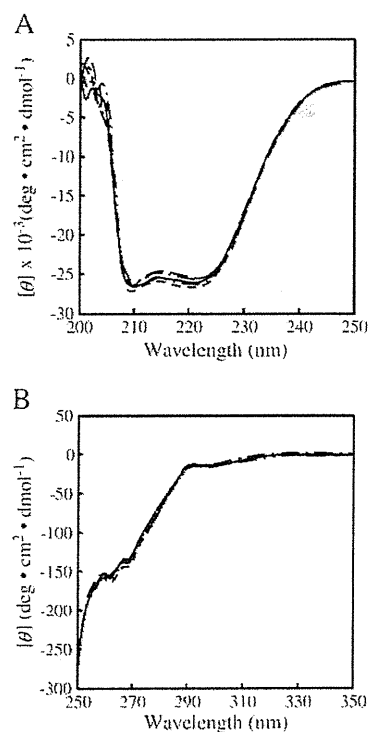


**Fig. 2.** CD spectra of rHSAs. A, far-UV and B, near-UV intrinsic spectra were recorded in the range from 200 to 250 nm and from 250 to 350 nm, respectively. The protein concentration was 5  $\mu\text{M}$  (far-UV) or 15  $\mu\text{M}$  (near-UV) in PBS at 25 °C, respectively. Spectra are shown for wild type (—), D63N (·····), A320T (-----), D494N (-----) and TM (-----).

9.0 min for A320T; 9.0 min for D494N; 8.9 min for TM). These data suggested that mutation and glycosylation neither affected the protein conformation nor the net charge of protein.

### 3.3. Pharmacokinetic properties and tissue distributions of Man-rHSAs

The fates of the  $^{111}\text{In}$ -Man-rHSAs administered to mice were evaluated by determining the radioactivity in plasma. As shown in Fig. 3A, the pharmacokinetic profiles for D63N and A320T were similar to wild-type rHSA. In contrast, D494N and TM-rHSAs were rapidly cleared from the blood circulation compared to other rHSAs, including wild-type protein. Using these data, pharmacokinetic analysis was carried out and plasma clearance ( $\text{CL}_{\text{tot}}$ ) were then estimated.  $\text{CL}_{\text{tot}}$  of wild type, D494N and TM-rHSAs were 0.8, 2.4 and 8.2 mL/h, respectively.

The tissue distributions of the Man-rHSAs were examined at 60 min after their administration. As shown in Fig. 3B, the tissue distribution patterns of the mutants, especially D494N and TM-rHSA were markedly changed compared to that of wild-type rHSA, which was largely present in the blood stream at 60 min. In the case of D494N and TM-rHSA, majority of the dose (50%, 65% for each mutant, respectively) after intravenous administration accumulated in the liver and small portions were also distributed to the kidney, lung and spleen.

Therefore, we further investigated the time course for the hepatic distribution of rHSAs (Fig. 3C). The hepatic uptake clearances ( $\text{CL}_{\text{uptake}}$  in liver) of D494N and TM-rHSA were 16 times and 47 times higher than that of wild-type rHSA ( $\text{CL}_{\text{uptake}}$  in liver; 0.13, 2.04 and 6.10 mL/h, for wild-type rHSA, D494N and TM-rHSA, respectively). These data clearly demonstrate that TM-rHSA was the most rapidly distributed and accumulated in the liver. Interestingly, the plasma

clearances and liver distributions of Man-rHSAs were dependent on the degree of oligosaccharide modification, which was in the order of TM-rHSA > D494N >> A320T = D63N. These results indicate that the oligosaccharide chain attached to D494N plays an important role in the pharmacokinetic characteristics of TM-rHSA, while the other two positions contribute additionally. We have also compared the hepatic distribution of both  $^{111}\text{In}$ -TM-rHSA and chemically modified  $^{111}\text{In}$ -Man-(12)-HSA (parenthesis means the number of sugars). No significant differences between TM-rHSA and Man-(12)-HSA were observed in the hepatic distribution at 60 min after administration (65% for TM-rHSA; 66% for Man-(12)-HSA) and in the hepatic uptake clearance. These results suggested that hepatic distribution of TM-rHSA was similar to that of chemically modified Man-(12)-HSA.

To determine whether MR is involved in this rapid hepatic uptake pathway, we carried out an *in vivo* study in which the hepatic distribution of TM-rHSA was estimated in the presence of a 100 times excess of chemically modified Man-(42)-BSA or 50 times excess of mannan, a well known substrate for MR. As shown in Fig. 3D, in the presence of Man-(42)-BSA or mannan, the hepatic distribution of TM-rHSA was decreased by about 90% or 50%, respectively, compared with that in the absence of these two MR substrates. On the other hand, no significant difference was observed in the presence of 100 times excess of chemically modified Gal-(55)-BSA, which is known to be taken up *via* asialoglycoprotein receptor expressed in liver parenchymal cells. Opanasopit et al. reported on *in vivo* inhibition experiments of  $^3\text{H}$ -Man-liposomes with excess amounts of Man-BSA and Man-liposome [21]. They reported that Man-BSA and Man-liposome inhibited the uptake of  $^3\text{H}$ -Man-liposomes by approximately 18% and 62%, respectively. In addition, the uptake of  $^{125}\text{I}$ -Man-BSA was suppressed by nearly half by an excess amount of Man-BSA in *in vitro*

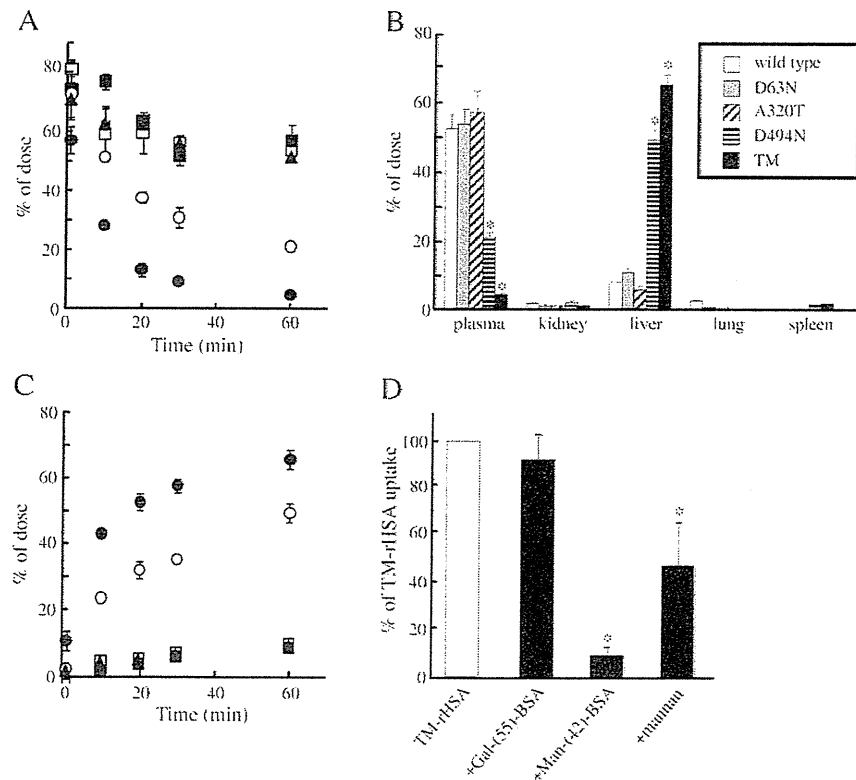


**Fig. 3.** A, Plasma concentration curve of rHSAs after 0.1 mg/kg of  $^{111}\text{In}$ -rHSAs were injected in tail vein of mice. Filled triangle, filled square, open square, open circle and filled circle represent for wild type, D63N, A320T, D494N and TM, respectively. B, tissue distributions of rHSAs at 60 min. C, Hepatic uptake of rHSAs after  $^{111}\text{In}$ -rHSAs were injected in tail vein of mice. Filled triangle, filled square, open square, open circle and filled circle represent for wild type, D63N, A320T, D494N and TM, respectively. Each value represents the mean  $\pm$  SD. \* $P < 0.01$  as compared with wild-type. D, Effect of 100 times excess of Gal-(55)-BSA or Man-(42)-BSA and 50 times excess of mannan on hepatic distribution of TM. Each value represents the mean  $\pm$  SD. \* $P < 0.01$  as compared with TM without inhibitor.

experiments using Kupffer cells [7]. In both studies, the investigators concluded that Man-liposome and Man-BSA were mainly taken up by the liver via MR. Thus, we conclude that MR plays pivotal role in the selective liver distribution of TM-rHSA. However, based on the present limited data, it is premature to conclude that other receptors such as scavenger receptors etc., are not involved in this process, and it must be necessary to examine the possibility of the contribution of other receptors.

#### 3.4. Uptake of TM-rHSA by liver cells

To investigate which specific cells are responsible for the liver uptake of Man-rHSA,  $^{111}\text{In}$ -labeled TM-rHSA was intravenously administrated to mice and the liver was then perfused with collagenase buffer, and separated into parenchymal cells and non-parenchymal cells. The findings indicate that more than 90% of the TM-rHSA is taken up by non-parenchymal cells (date not shown).

Furthermore, to examine which type of non-parenchymal cells are involved in the hepatic uptake of TM-rHSA, cellular uptake experiments were performed using primary-cultured endothelial cells and Kupffer cells. As a result, little uptake of  $^{125}\text{I}$ -labeled TM-rHSA was observed in endothelial cells (Fig. 4A), while Kupffer cells took up TM-rHSA, specifically (Fig. 4B). This result suggests that MR on Kupffer cells are mainly involved in the specific uptake of TM-rHSA. Considering the physicochemical and pharmacokinetic analysis data, among the four Man-rHSAs, TM-rHSA was selected as a candidate for use as a liver-selective carrier and was only used following *in vitro* and *in vivo* experiments.

#### 3.5. Cytoprotective effect of S-nitrosylated TM-rHSA after hepatic IR in rats

The over production of reactive oxygen species in Kupffer cells, the resident macrophages in the liver, during IR is one of the major causes of liver injury. Previous studies found that supplementation of NO to

the liver stimulated the induction of heme oxygenase-1 (HO-1) expression, which has been shown to have anti-inflammatory actions and protect mammalian cells against various types of free radical damage [22]. Thus, the supplementation of NO to the liver including Kupffer cells has received considerable attention as a new and novel strategy for inhibiting liver damage, especially IR injury.

To evaluate the potential of TM-rHSA as a NO traffic carrier to Kupffer cells, the effect of SNO-TM-rHSA on liver damage was examined using liver IR injury model rats. Since HSA contains only one free thiol group, i.e., Cys34, SNO-TM-rHSA was prepared by reacting TM-rHSA and isoamyl nitrite (described in the Materials and methods section). First, the S-nitroso content of TM-rHSA was estimated and found to be approximately 0.5 mol/mol protein which is higher than that of wild-type HSA (0.35 mol/mol protein). In a previous study, Ishima et al. reported that the administration of 0.01–0.1  $\mu\text{mol}/\text{rat}$  of SNO-wild-type rHSA suppressed liver injury [10]. Thus, in this *in vivo* study, to compare the suppressive effects on liver damage, the S-nitroso content of both TM-rHSA and wild-type rHSA was adjusted to 0.035  $\mu\text{mol}/\text{rat}$  and then injected into the liver injury model rats because the S-nitrosylation efficacies were different between two rHSAs, as discussed above.

The release of higher levels of liver enzymes AST and ALT was measured after the administration of SNO-TM-rHSA at the beginning of reperfusion. The effect of SNO-TM-rHSA was evaluated at 120 min after reperfusion, at which plasma AST and ALT levels were most increased [10]. As shown in Fig. 5A and B, SNO-wild-type rHSA effectively suppressed the IR injury. Interestingly, SNO-TM-rHSA inhibited IR injury more significantly than SNO-wild-type rHSA although an equivalent amount of NO was administrated. Wild-type and TM-rHSA (carrier alone) did not modify liver damage in this model (data not shown). These data suggest that SNO-TM-rHSA was more effective in delivering NO to Kupffer cells compared to SNO-wild-type HSA. To further compare the therapeutic efficacy with chemically modified Man-albumin, the effect of SNO-Man-(12)-HSA on hepatic IR injury was also examined in the same animal model. The results showed that the effect of SNO-Man-(12)-HSA after adjusting the S-nitroso content to 0.035  $\mu\text{mol}/\text{rat}$  on hepatic IR injury was not significantly different from that of SNO-TM-rHSA (data not shown), suggesting comparable efficacies between these two SNO-Man-albumins.

To confirm the effect of SNO-TM-rHSA, the total amount of NO derivatives, i.e.,  $\text{NO}_2^-$  and  $\text{NO}_3^-$  were measured after SNO-TM-rHSA administration *in vivo* because NO is very reactive and is readily converted to derivatives. As shown in Fig. 5C, the total amount of  $\text{NO}_2^-$  and  $\text{NO}_3^-$  was significantly increased as the result of SNO-TM-rHSA treatment, while TM-rHSA itself had no effect on the total amount of derivatives. This indicates that NO is effectively delivered to the liver via MR by TM-rHSA. These data clearly support the proposed mechanism for enhanced cytoprotective activity of SNO-TM-rHSA, as outlined above. As mentioned in Introduction section, it has been believed that an impaired production of NO is a significant contributor to the pathogenesis of hepatic IR injury. However, in the present study, the measurement of  $\text{NO}_x$  concentrations in the liver did not demonstrate an impaired NO production upon IR treatment (saline-treated group with or without IR treatment). Such inconsistency might be due to the increase of the expression level of iNOS at 120 min post reperfusion, because generally, NO production is decreased in ischemia condition accompanied by a decrease in the eNOS activity and is increased in reperfusion condition accompanied by an increase in the iNOS expression. In fact, impaired production of NO in hepatic IR injury has been deduced by the changes of eNOS activity and there is no study on the measurement of  $\text{NO}_x$  levels in hepatocellular during reperfusion, so far. Thus, to clarify this, it will be necessary to evaluate the time course of the changes of  $\text{NO}_x$  level during the hepatic IR injury in future. In any case, the replacement of NO has potent cytoprotection against IR liver injury. In fact, it has been reported that genetic deficiency of the eNOS significantly exacerbates IR injury in

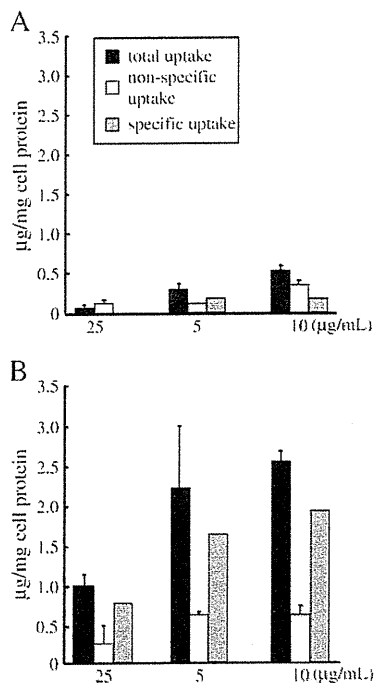
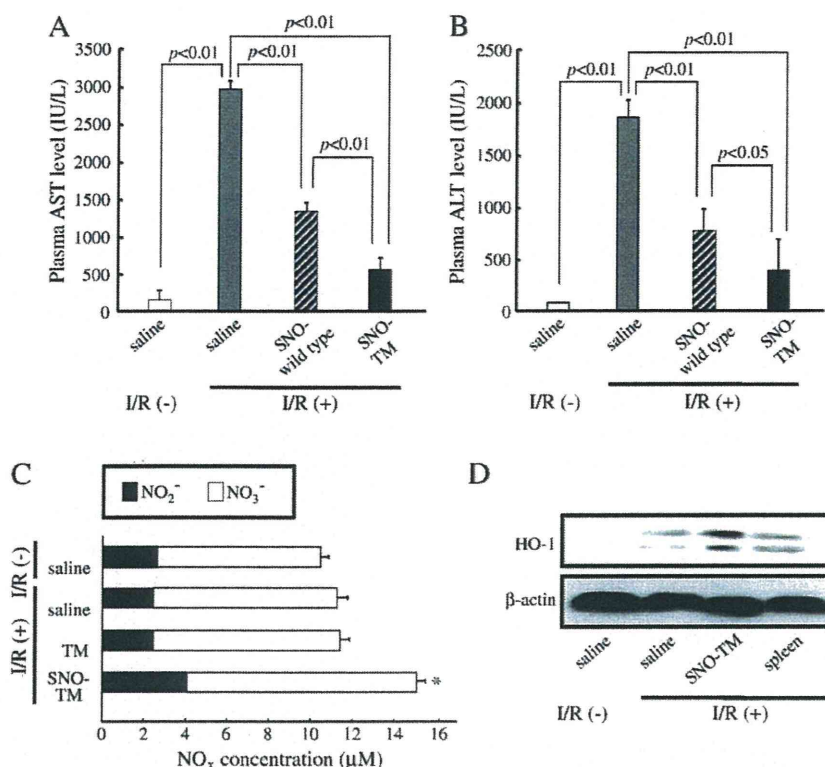


Fig. 4. Uptake of TM by liver non-parenchymal cells. A, Uptake of TM by endothelial cells and B, Uptake of TM by Kupffer cells. Specific uptake represents as total uptake minus nonspecific uptake. Total uptake and nonspecific uptake represents the mean  $\pm$  SD.



**Fig. 5.** Effect of SNO-TM on rat hepatic IR injury. SNO-wild type or SNO-TM was injected at beginning of reperfusion from the tail vein of rats after adjusting the S-nitroso content to 0.035  $\mu\text{mol}/\text{rat}$ . A, plasma AST level at 120 min after reperfusion. B, plasma ALT level at 120 min after reperfusion. Each value represents the mean  $\pm$  SD. \* $P < 0.01$  as compared with saline group with IR. C,  $\text{NO}_2^-$  and  $\text{NO}_3^-$  levels in liver. Liver was resected and homogenized at 120 min after reperfusion. Filled columns indicate liver  $\text{NO}_2^-$  levels and open columns indicate  $\text{NO}_3^-$  levels. Each value represents the mean  $\pm$  SD. \* $P < 0.05$  as compared with saline group and TM group with IR (+). D, HO-1 induction by SNO-TM treatment on rat hepatic IR injury. HO-1 level was determined at 120 min after reperfusion. HO-1 level in spleen was also determined as a positive control.

heart whereas overexpression of eNOS attenuates IR injury [23]. This is further supported by the evidence that pharmacological inhibition of NOS exacerbates myocardial I/R injury [24], whereas administration of the NO precursor L-arginine can ameliorate myocardial I/R injury. In addition, Ishima et al. [10] and Ikebe et al. [11] have shown that S-nitrosylated albumin or S-nitrosylated  $\alpha$ 1-protease inhibitor treatment significantly ameliorate liver damage against IR injury in rats.

### 3.6. Effect of SNO-TM-rHSA on HO-1 protein expression in the liver

To investigate the mechanism of the cytoprotective activity of SNO-TM-rHSA, HO-1 level was determined by Western blotting analysis (Fig. 5D). As previously reported, IR treatment caused the induction of hepatic HO-1 [11]. Interestingly, the administration of SNO-TM-rHSA further significantly induced HO-1 in IR model rats. This is in good agreement with both the cytoprotective activity (Fig. 5A and B) and  $\text{NO}_2^-$  and  $\text{NO}_3^-$  levels (Fig. 5C), suggesting that these are interrelated. These findings lead to the proposed mechanism in which the cytoprotective effects of SNO-TM-rHSA could be due to the induction of hepatic HO-1 levels by delivered NO molecules. Devey et al. also demonstrated that Kupffer cell depletion resulted in the loss of HO-1 expression and increased susceptibility to hepatic IR injury [25]. Targeted deletion of HO-1 rendered mice highly susceptible to hepatic IR injury. Consequently, they concluded that there is a critical role for tissue-resident macrophages in homeostasis following ischemic injury, and a co-dependence of HO-1 expression and tissue-resident macrophage differentiation. Since NO strongly stimulates HO-1 expression [22], the approach proposed herein which deliver the NO to Kupffer cells seems to be effective in hepatic IR injury. This will be more clearly demonstrated by the comparable analysis using SNO-Gal-

HSA or other glycosylated HSA. It is also suggested that the cytoprotective effects of S-nitrosothiol may involve multiple mechanisms, including 1) maintenance of tissue blood flow; 2) suppression of neutrophil infiltration; 3) reduction of apoptosis in the liver, in addition to 4) induction of HO-1, a cytoprotective enzyme [11].

### 3.7. Concluding remarks

In the present study, we successfully designed and genetically engineered TM-rHSA which has the ability to selectively deliver therapeutics to the liver via MR. To our knowledge, this is the first study to describe a genetically engineered rHSA with an oligosaccharide as a carrier for a drug delivery system and its therapeutic application. Our study showed that 1) among the four Man-rHSAs evaluated in this study, TM-rHSA was the most highly mannosylated and preserved the majority of the structural properties of wild-type HSA, 2) TM-rHSA was eliminated the most from the blood circulation and was then selectively taken up by the liver via MR on Kupffer cells, 3) SNO-TM-rHSA effectively delivered NO to the liver and exhibited a significant inhibitory effect against IR injury accompanied by the induction of HO-1. However, we have not explored the implication of the hepatic stellate cell, a non-parenchymal cell type in the liver that is known to have a crucial role when the liver is under hepatic fibrosis [26]. In addition, it was reported that an imbalance between endothelin and nitric oxide levels which results in the failure of hepatic microcirculation at the onset of reperfusion, and the activation of nuclear factor-kappa B in the liver which promotes proinflammatory cytokine and adhesion molecule synthesis contributed to the liver injury [27]. Therefore, examination of the effect of SNO-TM-rHSA on endothelin, inflammatory cytokine and adhesion molecule levels in addition to stellate cells activation should be one of the subjects of future investigation.

TM-rHSA was produced by inserting the consensus sequence for N-glycosylation using three genetically glycosylated HSA variants as a template and a *P. pastoris* expression system. Recombinant albumin products purified from yeast are currently coming on the commercial market. Basically, TM-rHSA can be produced by same bio-synthetic procedures using a recombinant albumin product. In addition, the results obtained here clearly demonstrated that this recombinant technique was able to be an alternative method for preparing Man-HSA without chemical modifications. Consequently, as compared to chemically modified Man-HSA, TM-rHSA can be prepared relatively homogeneous form and can be minimized the modification of reactive residues that attached the therapeutics and surface charges of HSA, which is favorable for producing a stable preparation. Furthermore, in the present study, only NO was tested as a therapeutic compound. However, this delivery system is not only limited to NO but has widespread applications for other liver therapeutics, such as drugs, cytokines, proteins, hormones etc. Therefore, TM-rHSA would be expected to become versatile carrier for liver-selective therapeutics.

### Acknowledgements

We acknowledge Ms. Tamami Kimura for their technical assistance. This research was supported [in part] by Grant-in-Aid for Scientific Research from Japan Society for the Promotion of Science (JSPS) (KAKENHI 18390051 and 21390177).

### References

- [1] V.T. Chuang, U. Kragh-Hansen, M. Otagiri, Pharmaceutical strategies utilizing recombinant human serum albumin, *Pharm. Res.* 19 (2002) 569–577.
- [2] L. Minchiotti, M. Campagnoli, A. Rossi, M.E. Cosulich, M. Monti, P. Pucci, U. Kragh-Hansen, B. Granel, P. Disdier, P.J. Weiller, M. Galliano, A nucleotide insertion and frameshift cause albumin Kenitra, an extended and O-glycosylated mutant of human serum albumin with two additional disulfide bridges, *Eur. J. Biochem.* 268 (2001) 344–352.
- [3] S.O. Brennan, T. Myles, R.J. Peach, D. Donaldson, P.M. George, Albumin Redhill (–1 Arg, 320 Ala→Thr): a glycoprotein variant of human serum albumin whose precursor has an aberrant signal peptidase cleavage site, *Proc. Natl Acad. Sci. USA* 87 (1990) 26–30.
- [4] J. Carlson, Y. Sakamoto, C.B. Laurell, J. Madison, S. Watkins, F.W. Putnam, Alloalbuminemia in Sweden: structural study and phenotypic distribution of nine albumin variants, *Proc. Natl Acad. Sci. USA* 89 (1992) 8225–8229.
- [5] R.J. Peach, S.O. Brennan, Structural characterization of a glycoprotein variant of human serum albumin: albumin Casebrook (494 Asp→Asn), *Biochim. Biophys. Acta* 1097 (1991) 49–54.
- [6] T.R. Gemmill, R.B. Trimble, Overview of N- and O-linked oligosaccharide structures found in various yeast species, *Biochim. Biophys. Acta* 1426 (1999) 227–237.
- [7] Y. Higuchi, M. Nishikawa, S. Kawakami, F. Yamashita, M. Hashida, Uptake characteristics of mannosylated and fucosylated bovine serum albumin in primary cultured rat sinusoidal endothelial cells and Kupffer cells, *Int. J. Pharm.* 287 (2004) 147–154.
- [8] Y. Yabe, M. Nishikawa, A. Tamada, Y. Takakura, M. Hashida, Targeted delivery and improved therapeutic potential of catalase by chemical modification: combination with superoxide dismutase derivatives, *J. Pharmacol. Exp. Ther.* 289 (1999) 1176–1184.
- [9] Y.R. Kuo, F.S. Wang, S.F. Jeng, B.S. Lutz, H.C. Huang, K.D. Yang, Nitrosoglutathione promotes flap survival via suppression of reperfusion injury-induced superoxide and inducible nitric oxide synthase induction, *J. Trauma* 57 (2004) 1025–1031.
- [10] Y. Ishima, T. Sawa, U. Kragh-Hansen, Y. Miyamoto, S. Matsushita, T. Akaike, M. Otagiri, S-Nitrosylation of human variant albumin Liprizzi (R410C) confers potent antibacterial and cytoprotective properties, *J. Pharmacol. Exp. Ther.* 320 (2007) 969–977.
- [11] N. Ikebe, T. Akaike, Y. Miyamoto, K. Hayashida, J. Yoshitake, M. Ogawa, H. Maeda, Protective effect of S-nitrosylated alpha(1)-protease inhibitor on hepatic ischemia-reperfusion injury, *J. Pharmacol. Exp. Ther.* 295 (2000) 904–911.
- [12] S. Matsushita, Y. Isima, V.T. Chuang, H. Watanabe, S. Tanase, T. Maruyama, M. Otagiri, Functional analysis of recombinant human serum albumin domains for pharmaceutical applications, *Pharm. Res.* 21 (2004) 1924–1932.
- [13] Y. Yabe, N. Kobayashi, M. Nishikawa, K. Mihara, F. Yamashita, Y. Takakura, M. Hashida, Pharmacokinetics and preventive effects of targeted catalase derivatives on hydrogen peroxide-induced injury in perfused rat liver, *Pharm. Res.* 19 (12) (2002) 1815–1821.
- [14] T.A. Scott, E.H. Melvin, The determination of dextran with anthrone, *Anal. Chem.* 25 (1953) 1656–1661.
- [15] D.J. Hnatowich, W.W. Layne, R.L. Childs, The preparation and labeling of DTPA-coupled albumin, *Int. J. Appl. Radiat. Isot.* 33 (5) (1982) 327–332.
- [16] S. Matsushita, V.T. Chuang, M. Kanazawa, S. Tanase, K. Kawai, T. Maruyama, A. Suenaga, M. Otagiri, Recombinant human serum albumin dimer has high blood circulation activity and low vascular permeability in comparison with native human serum albumin, *Pharm. Res.* 23 (5) (2006) 882–891.
- [17] M. Tabuchi, K. Umegaki, T. Ito, M. Suzuki, J. Tomita, M. Ikeda, T. Tomita, Fluctuation of serum NO(x) concentration at stroke onset in a rat spontaneous stroke model (M-SHRSP). Peroxynitrite formation in brain lesions, *Brain Res.* 949 (2002) 147–156.
- [18] K. Yamaoka, Y. Tanigawara, T. Nakagawa, T. Uno, A pharmacokinetic analysis program (multi) for microcomputer, *J. Pharmacobiodyn.* 4 (11) (1981) 879–885.
- [19] M. Murata, I. Tamai, Y. Sai, O. Nagata, H. Kato, Y. Sugiyama, A. Tsuji, Hepatobiliary transport kinetics of HSR-903, a new quinolone antibacterial agent, *Drug Metab. Dispos.* 26 (11) (1998) 1113–1119.
- [20] V. Blanchard, R.A. Gadkari, G.J. Gerwig, B.R. Leeflang, R.R. Dighe, J.P. Kamerling, Characterization of the N-linked oligosaccharides from human chorionic gonadotropin expressed in the methylotrophic yeast *Pichia pastoris*, *Glycoconj. J.* 24 (2007) 33–47.
- [21] P. Opanasopit, M. Sakai, M. Nishikawa, S. Kawakami, F. Yamashita, M. Hashida, Inhibition of liver metastasis by targeting of immunomodulators using mannosylated liposome carriers, *J. Control. Release* 80 (2002) 283–294.
- [22] C. Bouton, B. Demple, Nitric oxide-inducible expression of heme oxygenase-1 in human cells. Translation-independent stabilization of the mRNA and evidence for direct action of nitric oxide, *J. Biol. Chem.* 275 (42) (2000) 32688–32693.
- [23] S.P. Jones, J.J. Greer, A.K. Kakkar, P.D. Ware, R.H. Turnage, M. Hicks, R. van Haperen, R. de Crom, S. Kawashima, M. Yokoyama, D.J. Lefer, Endothelial nitric oxide synthase overexpression attenuates myocardial reperfusion injury, *Am. J. Physiol. Heart Circ. Physiol.* 286 (1) (2004) H276–H282.
- [24] R. Pabla, A.J. Buda, D.M. Flynn, D.B. Salzbberg, D.J. Lefer, Intracoronary nitric oxide improves postischemic coronary blood flow and myocardial contractile function, *Am. J. Physiol.* 269 (3Pt 2) (1995) H1113–H1121.
- [25] L. Devey, D. Ferenbach, E. Mohr, K. Sangster, C.O. Bellamy, J. Hughes, S.J. Wigmore, Tissue-resident macrophages protect the liver from ischemia reperfusion injury via a heme oxygenase-1-dependent mechanism, *Mol. Ther.* 17 (1) (2009) 65–72.
- [26] E. Broide, E. Klinowski, G. Koukoulis, N. Hadzic, B. Portmann, A. Baker, E. Scapa, G. Mieli-Vergani, Superoxide dismutase activity in children with chronic liver diseases, *J. Hepatol.* 32 (2) (2000) 188–192.
- [27] F. Serracino-Inglott, N.A. Habib, R.T. Mathie, Hepatic ischemia-reperfusion injury, *Am. J. Surg.* 181 (2) (2001) 160–166.

REVIEW ARTICLE

# Pharmacokinetic properties of hemoglobin vesicles as a substitute for red blood cells

Kazuaki Taguchi<sup>1</sup>, Toru Maruyama<sup>1,2</sup>, and Masaki Otagiri<sup>1,3</sup>

<sup>1</sup>Department of Biopharmaceutics, Kumamoto University, Kumamoto, Japan, <sup>2</sup>Center for Clinical Pharmaceutical Sciences, Graduate School of Pharmaceutical Sciences, Kumamoto University, Kumamoto, Japan, and <sup>3</sup>Faculty of Pharmaceutical Sciences, Sojo University, Kumamoto, Japan

## Abstract

The development of artificial oxygen carriers has attracted considerable recent interest because of the increasing cost of collecting and processing blood, public concerns about the safety of blood products, complications from blood transfusions, military requirements for increased volumes of blood during military conflicts, and a decrease in the number of new donors. To overcome these problems, perfluorocarbon-based oxygen carriers as well as acellular- and cellular-type, hemoglobin-based oxygen carriers have been developed for use as artificial oxygen carriers. Despite their extensive evaluation, including formulation and pharmacology, they have not been extensively used in clinical settings. One of the reasons for this is that their pharmacokinetics have not been well characterized. Artificial oxygen carriers require not only an acceptable level of physicochemical activity, but also clinical efficacy, as reflected by their retention in the circulation, and the absence of measurable accumulation in the body, if unexpected adverse effects are to be avoided. In this review, the pharmacokinetic properties of artificial oxygen carriers are discussed, with a focus on recent developments of our research related to the pharmacokinetic properties a cellular type of hemoglobin-based oxygen carrier.

**Keywords:** Artificial oxygen carrier, disposition, liposome, mononuclear phagocyte system, hemorrhagic shock, hepatic chronic cirrhosis, accelerated blood clearance phenomenon

## Introduction

In modern medical care, there is now little doubt that the transfusion of red blood cells (RBCs) is the gold standard for treatment of patients with massive hemorrhages and is currently in widespread use. Nevertheless, the potential for mismatching exists and infections by unrecognized pathogens, hepatitis, HIV, or West Nile virus, etc., are always a possibility. In addition, ensuring a steady supply of RBCs at a time of a disaster and during military conflicts could be difficult, because the lifetime of donated RBCs is limited to a short period. Further, a decrease in donors and an increase in recipients in some developed countries is also a problem. To overcome these problems, various artificial oxygen carriers have been under development worldwide. They can be divided into three major classes of materials, as follows: perfluorocarbon-based oxygen carriers, acellular-type, hemoglobin-based

oxygen carriers (HBOCs), and cellular-type HBOCs (Figure 1). Despite the many efforts to develop artificial oxygen carriers during the past several decades, some of them were, unfortunately, rejected for use as the result of preclinical and clinical trials. It is noteworthy that perfluorocarbon-based oxygen carriers and acellular-type HBOCs were excluded as possible candidates for artificial oxygen carriers, even though they proceeded to the stage of clinical trials.

One of the reasons that induced these adverse effects was due to the insufficient characterization of pharmacokinetics of these artificial oxygen carriers under various situations. The desirable features of artificial oxygen carriers as a substitute for RBCs is not only a long retention in the circulation to sustain its pharmacological effects, but also no bioaccumulation, which could lead to adverse effects. Unlike other drugs, because the dosage volume of

*Address for Correspondence:* Masaki Otagiri, Department of Biopharmaceutics, Graduate School of Pharmaceutical Sciences, Kumamoto University, 5-1 Oe-honmachi, Kumamoto 862-0973, Japan; Fax: +81-96-362-7690; E-mail: otagirim@gpo.kumamoto-u.ac.jp

*(Received 05 October 2010; revised 22 January 2011; accepted 24 January 2011)*

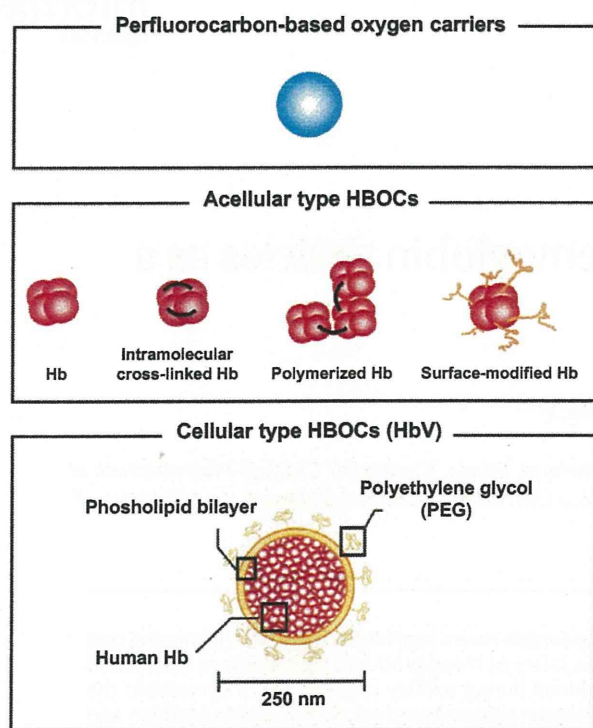


Figure 1. Schematic representation of perfluorocarbon-based oxygen carriers, acellular-type hemoglobin-based oxygen carriers (HBOCs), and cellular-type HBOCs (HbV). In the case of HbV, the surface is modified with polyethylene glycol (PEG) chains, and one HbV particle contains approximately 30,000 human Hb molecules obtained from outdated donated blood. The encapsulated Hb contains pyridoxal 5'-phosphate as an allosteric effector to regulate  $P_{50}$  to 25–28 torr. The lipid bilayer was comprised of a mixture of DPPC, cholesterol, and DHSG at a molar ratio of 5:5:1, and DSPE-PEG<sub>5000</sub> (0.3 mol%). The average particle diameter was regulated to approximately 250 nm.

an artificial oxygen carrier as an RBC substitute is more than a hundred times higher than that of other drugs, detailed information regarding the fate of an artificial oxygen carrier, including its constituent components, is needed, in order to predict unexpected adverse effects.

In this review, the pharmacokinetic properties of artificial oxygen carriers are discussed, with a focus on hemoglobin vesicles (HbVs), in which, among the current artificial oxygen carriers, its pharmacokinetic properties have been extensively characterized.

### Perfluorocarbon-based oxygen carriers

The perfluorocarbon-based oxygen carriers are characterized by a high gas-dissolving capacity, low viscosity, and chemical and biological inertness (Spahn and Kocian, 2003). They are molecules that are constructed from cyclic or straight-chain hydrocarbons, in which the hydrogen atoms are replaced by halogens, and are virtually immiscible with water and, therefore, must be emulsified prior to their use in intravenous applications (Pape and Habler, 2007). When perfluorocarbon emulsion droplets are injected into an organism, they are

rapidly taken up and slowly broken down by the mononuclear phagocyte system (MPS). After being degraded, the emulsion droplets are again taken up by the blood and transported to the lungs, where any unaltered molecules are excreted via exhalation (Spahn and Kocian, 2003; Jahr et al., 2007; Pape and Habler, 2007). However, perfluorocarbon-based oxygen carriers induced chronic pneumonitis due to their inefficient excretion from the body and their accumulation in the lung, a condition that persists for more than 1 year (Nose, 2004) (Table 1).

### Acellular-type HBOCs

The stroma-free hemoglobin (Hb) was developed for use as artificial oxygen carriers, but their systemic half-lives were too short (~0.5–1.5 hours) for them to effectively function as an optimal oxygen carrier (Savitsky et al., 1978). In addition, the Hb tetramers dissociate into their component  $\alpha\beta$  dimers, which are then eliminated by the kidneys, and induce renal toxicity (Creteur and Vincent, 2003). In an attempt to increase their systemic half-life and stability, the following three groups of chemically modified acellular-type HBOCs were developed: surface-modified Hb (Smani, 2008), intramolecularly cross-linked Hb (Chen et al., 2009), and polymerized Hb (Jahr et al., 2008) (Figure 1). These acellular HBOCs have improved systemic half-lives, in the range of 18–24 hours, and show decreased renal failure (Stowell, 2005) (Table 1). The polymerized bovine-derived Hb has been approved for limited use in South Africa (Lok, 2001). However, it was recently reported that the use of some acellular-type HBOCs leads to the development of myocardial lesions, as the result of decreasing nitric-oxide levels 24–48 hours after a single topload infusion (Burhop et al., 2004), leading to an increase in mortality rates in humans (Natanson et al., 2008).

### Hemoglobin vesicles

The hemoglobin vesicle (HbV) is a cellular-type HBOC that contains polyethylene glycol (PEG), in which phospholipid vesicles encapsulating highly concentrated human Hb are imbedded (Sakai et al., 2008) (Figure 1). The cellular structure of HbV (particle diameter: approximately 250 nm) most closely mimics the characteristics of a natural RBC, such as the cell-membrane function, which physically prevents the direct contact of Hb with the components of blood and the vasculature during its circulation. The characteristics of HbV are superior to donated RBCs in the following ways: the absence of viral contamination (Sakai et al., 1993; Abe et al., 2001), a long-term storage period of over 2 years at room temperature, and no blood-type antigens (Sakai et al., 2000; Sou et al., 2000) (Table 2). In addition, HbVs have the ability to transport oxygen equivalent to RBCs and also show improved survival in hemorrhagic shock animal models (Sakai et al., 2004b; Terajima et al., 2006; Sakai et al., 2009). Further, HbVs can control the release of oxygen by

adjusting the amount of allosteric effector and regulate rheological properties (e.g., viscosity and colloid osmotic pressure) to added human serum albumin (Sakai and Tsuchida, 2007). Therefore, HbV has attracted considerable attention as a possible new artificial oxygen carrier and has considerable promise for use in clinical settings.

We recently characterized the pharmacokinetic properties of HbV to clarify its efficacy and safety under conditions that mimic a clinical setting, as follows:

1. HbV was constructed from multiple components, including Hb, lipids, and iron from Hb. These components have potential risks for inducing harmful effects, when they accumulate at excessive levels in the body.
2. HbV is classified as a liposome preparation. It was previously reported that the pharmacokinetics of liposome-encapsulated amphotericin B differ between normal individuals and patients (Walsh et al., 1998; Bekersky et al., 2001).
3. The surface of HbV was modified by PEG to enhance the half-life in circulation and storage. It was recently reported that repeated injection of PEGylated liposomes influenced the pharmacokinetics of the second injected liposome (Dams et al., 2000; Ishida et al., 2003a).

Table 1. Pharmacokinetic properties of some artificial oxygen carriers.

	Perfluorocarbon-based oxygen carriers	Acellular-type HBOCs	Cellular-type HBOCs
Distribution	Liver, spleen	Liver	Liver, spleen
Metabolism	MPS	MPS	MPS
Excretion	Air	—	Internal Hb; urine outer membrane; feces
Half-life	~10 hours (rat)	~24 hours (rat)	30~40 hours (rat)
Existence in tissues	~1 year	—	~14 days

HBOCs, hemoglobin-based oxygen carriers; MPS, mononuclear phagocyte system.

Table 2. Physicochemical characteristics of HbV.

Parameter	
Particle diameter	ca. 250 nm
$P_{50}$	25–28 torr
Hb concentration	10 g/dL
MetHb	<3%
Colloid osmotic pressure	0 Torr
Intracellular Hb concentration	ca. 35 g/dL
Lipid composition <sup>a</sup>	DPPC/cholesterol/DHSG/DSPE-PEG <sub>5000</sub>
Stability for storage at room temperature	Over 2 years, purged with N <sub>2</sub>

<sup>a</sup>DPPC, 1,2-dipalmitoyl-*sn*-glycero-3-phosphatidylcholine; DHSG, 1,5-bis-*O*-hexadecyl-*N*-succinyl-L-glutamate; DSPE-PEG<sub>5000</sub>, 1,2-distearoyl-*sn*-glycero-3-phosphatidyl-ethanolamine-*N*-PEG.

For these reasons, it becomes necessary to clarify the pharmacokinetic properties of HbV in various animal models and under conditions of repeated injection, if RBCs are to be used as a substitute in the future. For this purpose, 1) the disposition of HbVs was examined using isotope tracer techniques. In these experiments, <sup>125</sup>I-HbV, enclosed in HbVs, was radiolabeled with <sup>125</sup>I, and the lipid component vesicles of HbVs was radiolabeled with <sup>3</sup>H; 2) a pharmacokinetic study of HbVs in a rat model of hemorrhagic shock and hepatic chronic cirrhosis; 3) the repeated injection in normal and the hemorrhagic shock rat model; and 4) animal scale-up using an allometric equation, were conducted.

Some highlights of recent developments of our research related to the pharmacokinetic properties of HbV are discussed below.

### The prior pharmacokinetic characteristics of HbV to stroma-free Hb

Two requirements need to be satisfied if HbV is to be accepted for use as an artificial oxygen carrier. For clinical applications, HbVs must have not only an acceptable physicochemical activity, but also must be safe for use in the clinic. In the latter case, the supply of oxygen tissues is one of the most important factors in sustaining the clinical effect of HbVs (Takaori, 2005). To fulfill these requirements, a prolonged half-life is a required property for HbVs.

We recently demonstrated that the half-life of HbV in mice was 30 times higher than that of stroma-free Hb at a dose rate of 1 mg Hb/kg (Table 3). Moreover, a dose-dependent study clearly showed that the plasma concentration curve and half-life of HbV in mice and rats increased with increasing doses of HbV (Figure 2, half-life; rats: 8.8±0.7, 11.5±0.3, and 30.6±4.0 hours at doses of 10, 200, and 1,400 mg Hb/kg, respectively; mice: 3.1±3.1, 3.6±1.3, 7.2±3.1, and 18.8±1.3 hours at doses of 1, 10, 200, and 1,400 mg Hb/kg, respectively) (Taguchi et al., 2009b).

These superior pharmacokinetic characteristic of HbV, compared to stroma-free Hb, could reflect their physicochemical differences, such as particle diameter, the absence or presence of a membrane structure, and PEG modification. In physiological conditions, free Hb that is released from ruptured RBC is rapidly bound to

Table 3. Pharmacokinetic parameters for HbV after the administration of <sup>125</sup>I-Hb and <sup>125</sup>I-HbV in mice at a dose of 1 mg Hb/kg.

	<sup>125</sup> I-Hb	<sup>125</sup> I-HbV	<i>p</i>
$t_{1/2}$ (hr)	0.1±0.1	3.1±1.0	<0.01
AUC (hr <sup>2</sup> % of dose/mL)	7.9±3.9	29.4±9.2	<0.001
CL (mL/hr)	12.7±2.1	3.4±0.1	<0.001
V (mL)	2.6±0.3	2.3±0.1	N.S.

$t_{1/2}$ , half-life; AUC, are under the plasma-concentration versus time curve; CL, clearance; V, distributed volume; N.S., not significant.



haptoglobin (Hp), which promotes CD163 recognition in the liver (Kristiansen et al., 2001). When the Hb concentration exceeds the Hp-binding capacity, unbound Hb is removed by filtration through the kidney. Therefore, the reduction in HbV distribution in the liver and kidney could be due to the encapsulation of Hb by liposomes because this might not only suppress the binding of internal Hb to Hp, but also inhibit renal glomerular filtration. In fact, it was observed that the distribution of HbV in the liver and kidney was suppressed, compared with that of stroma-free Hb (Taguchi et al., 2009b). Moreover, the membrane surface modification by PEG also contributed to the increased half-life of HbV. In general, it is well-known that liposomes are scavenged and degraded by the MPS, such as Kupffer cells or macrophages in the spleen (Kiwada et al., 1998). PEGylation is a useful method for suppressing the capture of MPS, and the majority of the recently developed liposome formulations are modified with PEG (Noble et al., 2006; Sou et al., 2007; Okamura et al., 2009). Therefore, the modification of HbV with PEGylation is important to not only stabilize for a long-time storage, but also to maintain the good retention in the circulation. These balanced physicochemical activities result in a longer retention in the circulation, compared to stroma-free Hb and acellular-type HBOCs (Goins et al., 1995; Chang et al., 2003; Lee et al., 2006).

### The disposition of HbV components

In clinical situations as a substitute of RBCs, massive amounts of HbV are typically given to patients. As a result, its associated components, including Hb, lipids from Hb,

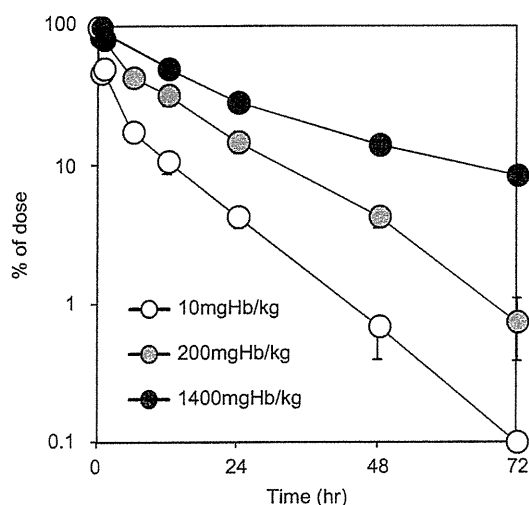


Figure 2. Dose-dependent plasma concentration curve of  $^{125}\text{I}$ -HbV after administration of  $^{125}\text{I}$ -HbV in rats. All rats received a single injection of  $^{125}\text{I}$ -HbV at a dose of 10 (open squares), 200 (gray circles), and 1,400 mg Hb/kg (closed circles) containing 5% rHSA. At each time point (0.05, 0.5, 1, 6, 12, 24, 48, and 72 hours) after the  $^{125}\text{I}$ -HbV injection, blood samples were collected from the tail vein, and a plasma sample was obtained. Each point represents the mean  $\pm$  SD ( $n=3-5$ ).

could result in undesirable consequences in the systemic circulation and organs during its metabolism and disposition. Such an extraordinary load of HbV components could result in the accumulation of components in the blood or organs, and has the potential to cause a variety of adverse effects, as follows: 1) high levels of lipid components, especially cholesterol, in the bloodstream, which are risk factors for kidney disease, arterial sclerosis, and hyperlipidemia (Grone and Grone, 2008); 2) Hb induces renal toxicity by dissociation of the tetramic Hb subunits into two dimers (Parry, 1988); and 3) free iron can trigger tissue damage induced by the Fenton reaction, which is mediated by heme (iron) (Balla et al., 2005). Therefore, it becomes necessary to clarify whether HbV and its components have favorable metabolic and excretion profiles. In order to investigate the disposition of each HbV component, Hb, enclosed in HbV, was radiolabeled with  $^{125}\text{I}$  ( $^{125}\text{I}$ -HbV) or cholesterol, in the lipid component vesicles of HbV, was radiolabeled with  $^3\text{H}$  ( $^3\text{H}$ -HbV).

In the blood circulation, HbV typically maintains an intact structure for periods of up to 72 hours after injection, because similar plasma concentration curves for  $^{125}\text{I}$ -HbV were observed for  $^3\text{H}$ -HbV in rats (Figure 3A), and the pharmacokinetic parameters were also consistent between them (half-life:  $30.6 \pm 4.0$ ,  $30.9 \pm 4.7$  hours; clearance in plasma:  $0.46 \pm 0.04$ ,  $0.41 \pm 0.02$  mL/h, for  $^{125}\text{I}$ - and  $^3\text{H}$ -HbV, respectively). Moreover,  $^{125}\text{I}$ -HbV and  $^3\text{H}$ -HbV were mainly distributed in the liver and spleen (Figure 3B). Because HbV possesses a liposome structure, it would be predicted that it would be captured by the MPS in the liver and spleen (Kiwada et al., 1998). In fact, a previous *in vitro* study clearly demonstrated that HbV was specifically taken up and degraded in RAW 264.7 cells, which has been used as an alternative to Kupffer cells, but this was not the case for parenchymal and endothelial cells (Taguchi et al., 2009b). In addition, the uptake clearance ( $\text{CL}_{\text{uptake}}$ ) in the liver and spleen were also similar between the two labeled preparations (liver:  $1,141 \pm 142$ ,  $1,098 \pm 123$ ; spleen:  $619 \pm 40$ ,  $518 \pm 89$   $\mu\text{L}/\text{h}$ , for  $^{125}\text{I}$ -HbV and  $^3\text{H}$ -HbV, respectively). However,  $^{125}\text{I}$  was more rapidly eliminated from each organ, and the activity essentially disappeared within 7 days. On the other hand, the elimination of radioactive  $^3\text{H}$  was delayed, compared to that of  $^{125}\text{I}$ , but nearly disappeared after 14 days. These data indicate that HbV is mainly distributed to the liver and spleen in the form of intact HbV, and that it was degraded by the MPS. In order to identify the excretion pathway of HbV, the levels of radioactivity of  $^{125}\text{I}$  and  $^3\text{H}$  in the urine and feces were measured. The radioactive  $^{125}\text{I}$  was excreted mainly in the urine, whereas the majority of the  $^3\text{H}$  was excreted in the feces. Based on the above findings, the disposition of HbV and its components, after circulating in the form of stable HbV, are distributed to the liver and spleen, where they are degraded by the MPS. Finally, the enclosed Hb and outer lipid components were mainly eliminated to the urine and feces, respectively, in the same manner as endogenous substances (Figure 4). Similar results were also reported in mice and rabbits (Sou et al.,

2005; Taguchi et al., 2009b); these results indicate that HbV and its components have favorable metabolic and excretion profiles in mammalian species. In addition, the plasma concentration curve for heme (iron) derived from HbV was similar to that for  $^{125}\text{I}$ -HbV and  $^3\text{H}$ -HbV in mice (Taguchi et al., 2009b). Moreover, no significant differences in the ratio of the mercapt- (i.e., nonoxidized form) to the nonmercapt-form (i.e., oxidized form) of rat serum albumin, which serves as a marker of oxidative stress in the circulation system (Kadowaki et al., 2007; Shimoishi et al., 2007), were found between HbV and the saline administration groups for periods of up to 7 days after administration. These results suggest that excess free heme (iron) derived from HbV is not released in the plasma. However, the issue of the disposition of several HbV components, including PEG and phospholipid, was not clarified. It is also possible that these components in HbV are also metabolized and excreted in the same manner as endogenous substances, but further study will be needed to demonstrate this fact.

### Pharmacokinetic properties of HbV under conditions of hemorrhagic shock

It is well known that clinical conditions can have an effect on the pharmacokinetics of numerous drugs (Abernethy et al., 1981; Turck et al., 1996). For example, it has demonstrated that the pharmacokinetics of liposome-encapsulated amphotericin B differ between normal individuals and patients in a clinical trial stage (Walsh et al., 1998; Bekersky et al., 2001). Consequently, it is possible that the pharmacokinetics of HbV would be also altered in the situation of a massive hemorrhage caused by injury, accidental blood loss, or a major surgery. To clarify this, we investigated the changes in HbV pharmacokinetics using a rat model of hemorrhagic shock induced by massive hemorrhage.

As shown in Figure 5, the retention of HbV in plasma under this condition was shorter, and the half-life of HbV was reduced significantly—by 0.66-fold—compared with the half-life of HbV in normal rats ( $30.6 \pm 4.0$ ,  $18.1 \pm 3.7$  hours, for normal and hemorrhagic shock, respectively). At a glance, this appears to not be a desirable situation for the therapeutic use of HbV, because an important determinant of HbV efficacy is a long retention in the blood circulation. However, the distribution volume of the central compartment of HbV ( $V_c$ ) was identical between normal and hemorrhagic shock rats, whereas the distribution volume of the peripheral compartment ( $V_p$ ) in hemorrhagic shock rats was nearly 2-fold greater than that of normal rats (Figure 5, insert). Moreover, the time-course tissue distribution of HbV in the hemorrhagic shock rats was greater than normal rats. These findings indicate that the shorter half-life in hemorrhagic shock rats appears to be the result in an apparent reduction in HbV in the arteriovenous circulation. If this enhanced tissue distribution of HbV might be derived by an increased scavenging of HbV by the MPS, such as by

Kupffer cells, red pulp zone splenocytes, and mesangial cells (Sakai et al., 2004a), it would not be expected to show significant pharmacological efficacy as an oxygen carrier, because HbV must maintain an intact structure to maintain its oxygen-carrying capacity. However, the pharmacological effect in the hemorrhagic shock model animal was significantly increased by the HbV treatment, similar to that for an RBC treatment (Sakai et al., 2004b; Terajima et al., 2006; Sakai et al., 2009). In addition, the amount of excretion into the urine, which is the major elimination pathway, did not differ between normal and hemorrhagic shock rats in our pharmacokinetic study. Therefore, HbV appears to be transferred from the arteriovenous blood to organ capillary beds as an intact structure, and is not excessively captured and metabolized by the MPS. These findings support the conclusion

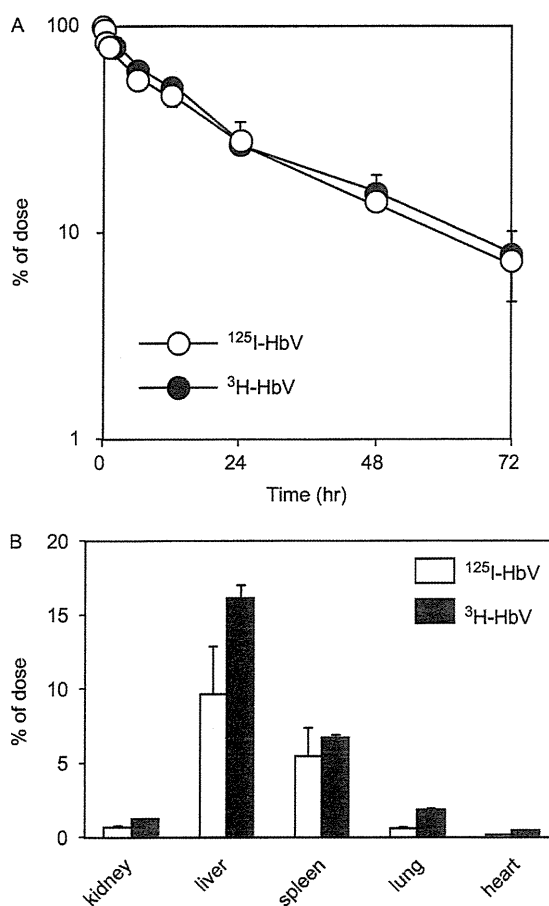


Figure 3. (A) Time course for the plasma level of  $^{125}\text{I}$ -HbV (open circles) and  $^3\text{H}$ -HbV (filled circles) after administration to rats. SD rats received a single injection of  $^{125}\text{I}$ -HbV or  $^3\text{H}$ -HbV to the tail vein at a dose of 1,400 mg Hb/kg. Blood was collected from the tail vein under ether anesthesia, and a plasma sample was obtained. Each point represents the mean  $\pm$  SD ( $n=5$ ). (B) Tissue distributions of  $^{125}\text{I}$ -HbV (open bars) and  $^3\text{H}$ -HbV (filled bars) at 24 hours after administration to mice. SD rats received a single injection of  $^{125}\text{I}$ -HbV or  $^3\text{H}$ -HbV from the tail vein at a dose of 1,400 mg Hb/kg. At 24 hours after injection, each organ was collected. Each bar represents the mean  $\pm$  SD ( $n=5$ ).

that HbV is pharmacologically efficacious in a rat model of HS induced by massive hemorrhage (Sakai et al., 2004b, 2009) is retained for a sufficiently long period to meet oxygen-delivery demands until autologous blood volume and oxygen-carrying capacity are restored.

### Pharmacokinetic properties of HbV in the condition with chronic liver failure

As mentioned above, the liver is the determinant for the pharmacokinetic properties of HbV, because HbV is mainly degraded by Kupffer cells, and the lipid components of HbV, especially cholesterol, are excreted to the feces via biliary excretion (Sakai et al., 2001; Taguchi et al., 2009b). Consequently, HbV can be classified as a hepatically cleared and excreted drug. In the case of other hepatically cleared and excreted drugs, some are contraindicated for a person with a hepatic injury. Because hepatic impairment affects the pharmacokinetics of drugs, including their metabolism and excretion (Okumura et al., 2007), these changes have the potential

to induce toxicity and accumulate in the body, subsequently causing unexpected adverse effects. Thus, if HbV and its components show the changes of pharmacokinetic properties under conditions of liver failure, it may also be contraindicated for a person with liver impairment under such conditions. Therefore, we investigated the pharmacokinetic properties of HbV using a chronic cirrhosis rat model with fibrosis induced by the administration of carbon tetrachloride, which is categorized as Child-Pugh grade B (Taguchi et al., 2011b).

After the administration of HbV to chronic cirrhosis rats, the plasma concentration of HbV varied widely among individuals, similar to their liver function. To clarify the effect of hepatic impairment on the plasma concentration of HbV, the clearance and the area under the concentration-time curve values for HbV, as calculated from the plasma concentration curve, were plotted against plasma aspartate aminotransferase (AST) levels. As a result, a good, negative correlation was found for the clearance of HbV with changes in plasma AST levels. In addition, the hepatic distribution of HbV was negatively

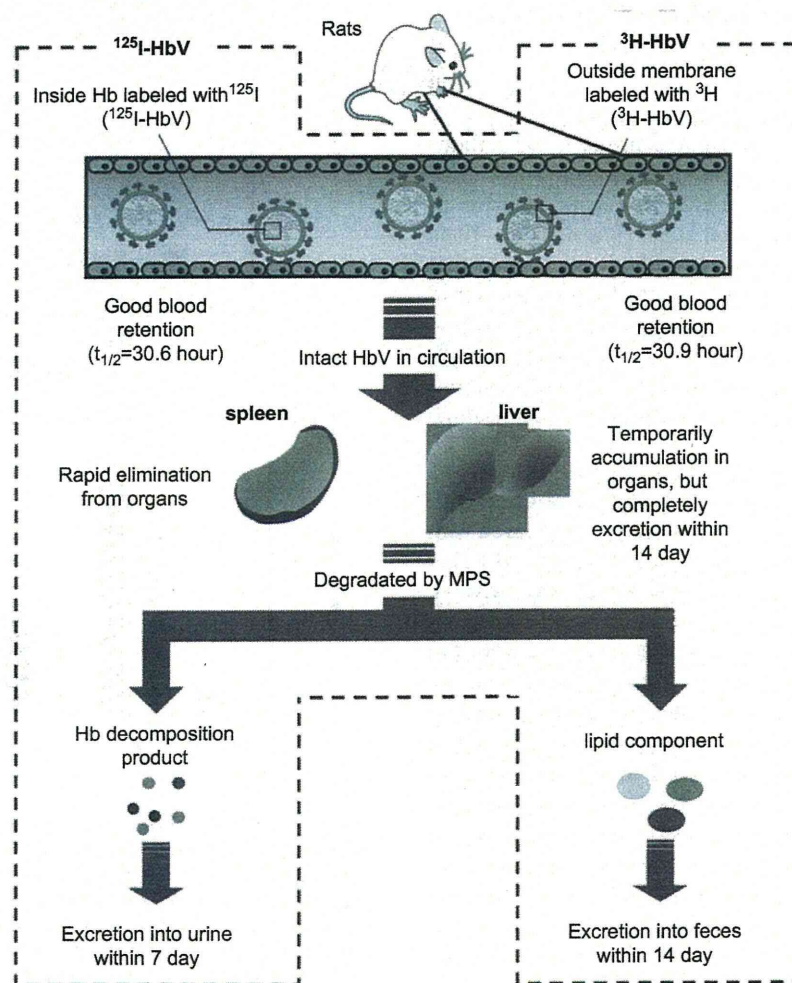


Figure 4. Representation of a sequence of HbV disposition, metabolism, and excretion from pharmacokinetic examinations, using  $^{125}\text{I}$ -HbV and  $^3\text{H}$ -HbV. After circulating in the form of stable HbV, it is distributed to the liver and spleen, where it is degraded by MPS. Finally, the enclosed Hb and outer lipid components are mainly eliminated to the urine and feces, respectively.

correlated with plasma AST levels, but this was not found for the spleen. Moreover, carbon clearance, which serves as a measure of phagocyte activity in Kupffer cells (Zweifach and Benacerraf, 1958), was also negatively correlated with plasma AST levels. Therefore, the changes in HbV pharmacokinetic properties were significantly influenced by a reduction in liver function and were especially dependent on a decrease in phagocyte activity by Kupffer cells in the chronic cirrhosis rat.

In addition, the excretion of lipid components (e.g., cholesterol) in feces was also negatively correlated with plasma AST levels. The cholesterol of the vesicles should reappear in the blood mainly as lipoprotein cholesterol after entrapment by Kupffer cells and should then be excreted in the bile after entrapment of the lipoprotein cholesterol by the hepatocytes (Kuipers et al., 1986). Therefore, the extent of damage to parenchymal cells also affects the pharmacokinetic properties of HbV components. Such a suppressed elimination of HbV components may have an impact on their tissue accumulation. However, the lipid components, especially cholesterol, nearly completely disappeared from organs after 7 days in the chronic cirrhosis rat. Further, our recent study showed that the plasma levels of other lipid components, such as phospholipids, was temporarily increased after the administration of HbV at a dose of 1,400 mg Hb/kg in the chronic cirrhosis rat, but recovered to baseline levels within 14 days (Taguchi et al., 2010). In addition, if the metabolic and excretion performance of HbV were reduced by chronic cirrhosis, tissue damage could be induced, resulting in a change in blood biochemical parameters. However, the morphological changes in organs were minimal (Figure 6), and only negligible changes in plasma biochemical parameters were

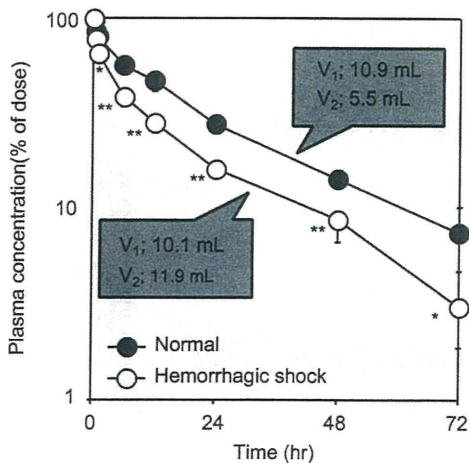


Figure 5. Relative plasma concentration of <sup>125</sup>I-HbV after administration of 1,400 mg Hb/kg via injection of normal (filled circles) or hemorrhagic shock rats (open circles). After inserting polyethylene catheters into the left femoral artery, SD rats received a single injection of <sup>125</sup>I-HbV to the left femoral artery at a dose of 1,400 mg Hb/kg. Blood was collected from the tail vein under ether anesthesia, and a plasma sample was obtained. Each point represents the mean ± SD (n=5).

observed after an HbV injection at a dose of 1,400 mg Hb/kg in the chronic cirrhosis rats. Based on these findings, it can be concluded that the pharmacokinetics of HbV were altered by hepatic impairment, and these changes can be attributed to a decrease in Kupffer-cell phagocyte activity (Figure 7). However, HbV and its components were completely metabolized and excreted within 14 days, and a temporary accumulation did not cause any obvious adverse effects.

### Pharmacokinetic properties of HbV after repeated administration in mice

HbV is modified by PEG to prolong its half-life and prevent aggregation during long-term storage, etc., as well

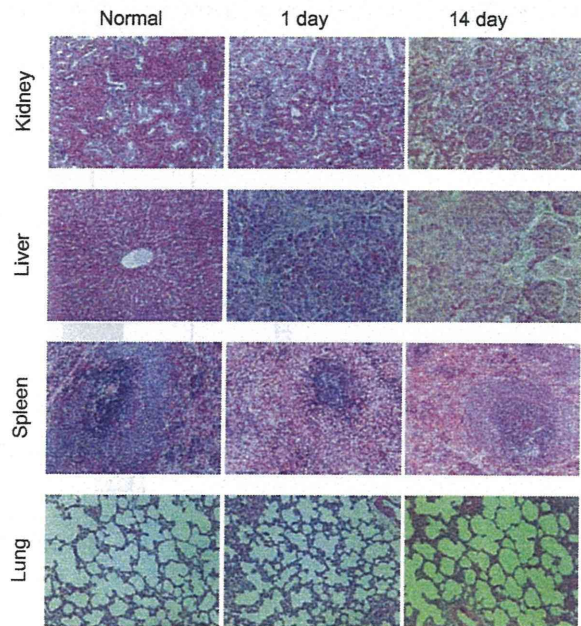


Figure 6. Light micrographs of kidney, liver, spleen, lung, and heart in CCl<sub>4</sub>-treated rats after an HbV injection stained with hematoxylin and eosin (X100). Chronic cirrhosis model rats received a single injection of HbV at a dose of 1,400 mg Hb/kg. No noticeable changes were observed in all organs after HbV injection.

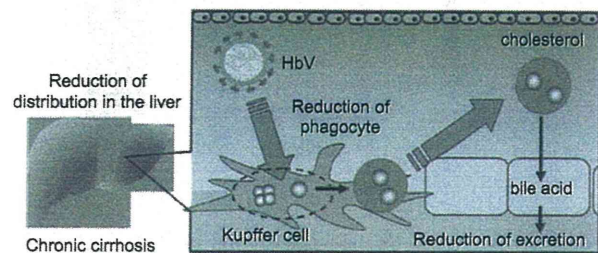


Figure 7. Representation of the pharmacokinetic properties of HbV in a rat model of chronic cirrhosis. Hepatic impairment altered the pharmacokinetic properties of HbV, such as blood retention, hepatic distribution, and fecal excretion, by a reduction in Kupffer cell phagocyte activity and damage to parenchymal cells.

as other liposome preparations. However, it was reported that repeated intravenous injection of PEGylated liposomes causes the second dose of liposomes to lose their long-circulating characteristics and accumulate extensively in the liver, when they are administrated at the same dose for the second time to the same animal within a several-day interval [referred to as the accelerated blood clearance (ABC) phenomenon] (Dams et al., 2000; Ishida et al., 2003a). The time frame between administration of the first and second dose for this to occur depends on the experimental animal, for example, 4–5 days for the rat and 7–10 days for the mouse. Repeated HbV injections of high doses would be routinely used in clinical practice for an RBC substitute. Therefore, the possibility remains that repeated injections of HbV could induce the ABC phenomenon in a clinical situation. If the ABC phenomenon were induced by repeated injections, then

the pharmacological action of HbV could be influenced. Therefore, we investigated the issue of whether HbV induces the ABC phenomenon in mice at a low dose (0.1 mg Hb/kg), a dose that is generally known to induce the ABC phenomenon (Ishida et al., 2003a), or a high dose (1,400 mg Hb/kg), the putative dose for clinical use.

At 7 days, in which the ABC phenomenon in mice is typically observed the most strongly (Ishida et al., 2003b), after the first injection of nonlabeled HbV (0.1 or 1,400 mg Hb/kg), the mice received  $^{125}\text{I}$ -HbV. At a low dose (0.1 mg Hb/kg), plasma HbV in the second injection was rapidly cleared, compared to that in the first injection. In contrast, at a high dose (1,400 mg Hb/kg), the pharmacokinetics of HbV were negligibly affected by repeated injections (Taguchi et al., 2009c). The liver and spleen are the major distribution organs for HbV (Taguchi et al., 2009b) and are related to the induction of

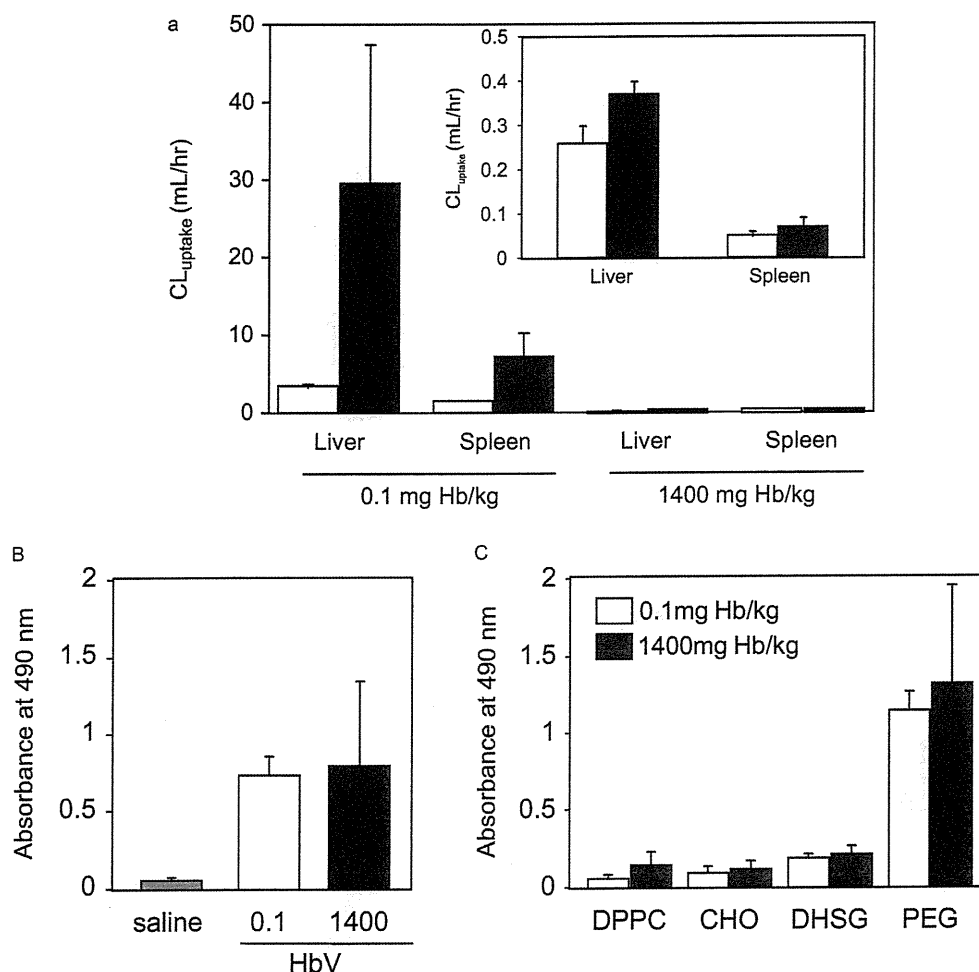


Figure 8. (A) Uptake clearance of HbV in the liver and spleen after 1 or 2 injections of  $^{125}\text{I}$ -HbV. Uptake clearance for each organ was calculated by integration plot analysis at designated times from 1 to 30 minutes after injection. Each bar represents the mean  $\pm$  SD ( $n=4$ ). (B) Determination of IgM against HbV after a single intravenous injection of saline (gray bars), HbV at a dose of 0.1 mg Hb/kg (open bars), or 1,400 mg Hb/kg (closed bars) in mice. (C) Determination of the specific recognition site of IgM against HbV after a single intravenous injection of HbV at a dose of 0.1 mg Hb/kg (open bars) or 1,400 mg Hb/kg (closed bars) in mice. DdY mice were injected with saline or HbV (0.1 or 1,400 mg Hb/kg) containing 5% rHSA to the tail vein. At 7 days after an injection of saline or HbV, blood was collected from the inferior vena cava, and plasma was obtained. IgM against HbV and each lipid component were detected by ELISA. Each bar represents the mean  $\pm$  SD ( $n=4$ ).

the ABC phenomenon (Ishida et al., 2008). At a low dose, the hepatic and splenic  $CL_{\text{uptake}}$  for the second injection was 8.5 and 4.5 times higher than that for the first injection, respectively (Figure 8A), whereas at a high dose, the hepatic and splenic  $CL_{\text{uptake}}$  for the second injection was little changed, compared to that for the first injection (Figure 8A, insert). In addition, Ishida et al. proposed a mechanism for the ABC phenomenon as follows: Immunoglobulin M (IgM), produced in the spleen by the first injection with PEGylated liposomes, selectively binds to the PEG on the second injected PEGylated liposome, and subsequent complement activation by IgM results in an accelerated clearance and enhanced hepatic uptake of the second injected PEGylated liposome (Ishida et al., 2006a, 2006b). Therefore, we examined whether IgM against HbV is elicited by an initial injection of saline or HbV at a low or high dose. At 7 days after the HbV injection, IgM against HbV appeared at both the low and the high dose (Figure 8B). Moreover, the specific recognition site of IgM against HbV strongly bound to DSPE-PEG, and other lipid components (DPPC, cholesterol, and DHSG) were negligible at both the low and high dose (Figure 8C). These results indicate that repeated injections of HbV to mice at a dose of 1,400 mg Hb/kg did not appear to induce the ABC phenomenon, even though the plasma levels of IgM against HbV are elevated. Therefore, these data suggest that a clinical dose of HbV is not likely to induce the ABC phenomenon due to the saturation of phagocytic processing by the MPS.

### Pharmacokinetic properties of HbV after repeated administration in hemorrhagic shock model rats

Because there are limited data available for the ABC phenomenon under various disease conditions, we also investigated whether the ABC phenomenon would be induced in the rat model of hemorrhagic shock induced by a massive hemorrhage, when HbV is injected at a dose of 1,400 mg Hb/kg at hourly intervals, typical conditions for transfusions of patients with massive hemorrhage.

The plasma concentration of HbV was prolonged in the second injection, compared with the first injection, and it was recovered to that in normal rats (Figure 9A). As mentioned above, Ishida et al. reported that a dosing interval of approximately 5 days induced the ABC phenomenon in rats, accompanied by the production of antiliposome IgM, which elicits a response by the spleen (Ishida et al., 2006b; Wang et al., 2007). Therefore, the inhibition of anti-HbV IgM production by short intervals appears to prevent induction of the ABC phenomenon. In fact, anti-HbV IgM was detected at 5 days after the administration of HbV to normal rats at a dose of 0.1 mg Hb/kg, but was not detected at 1 hour after HbV administration to hemorrhagic shock rats at a dose of 1,400 mg Hb/kg (Figure 9B). Therefore, it appears that

the repeated administration of HbV under conditions of hemorrhagic shock has negligible effect on the pharmacokinetics of HbV, when short dosing intervals are involved. However, our recent study showed that the repeated injection of HbV induced the ABC phenomenon in the case of a longer dosing interval (4 and 7 days) accompanied by the production of antiliposome IgM and increased phagocyte activity (Taguchi et al., 2011a). Therefore, in a clinical setting, it would be necessary to consider the dosing regimen and interval for patients with hemorrhagic shock in the base where a longer dosing interval was used.

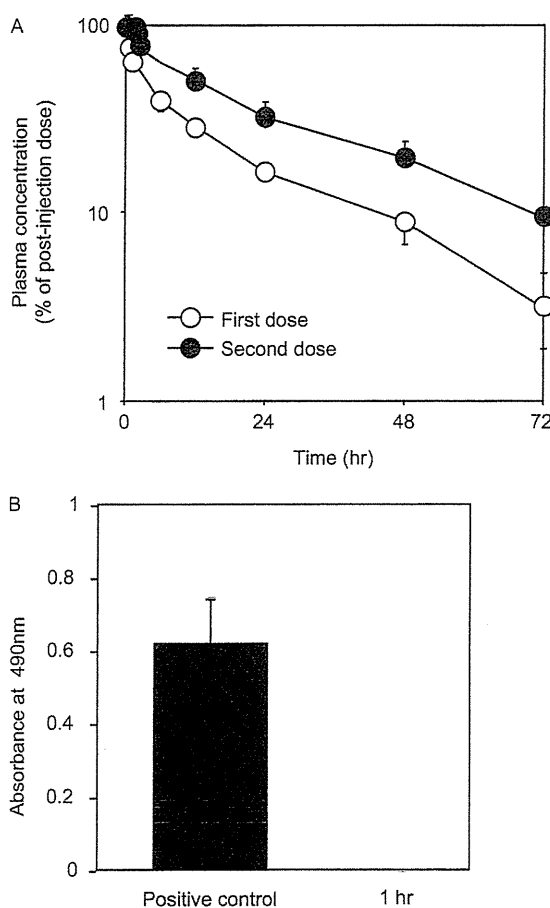


Figure 9. (A), Plasma concentration of  $^{125}\text{I}$ -HbV as the percent of postinjection dose after the first (open symbol) or second dose (filled symbol) of  $^{125}\text{I}$ -HbV to hemorrhagic shock rats at a dose of 1,400 mg Hb/kg for each injection. Each point represents the mean  $\pm$  SD ( $n=5$ ). Plasma concentration percentage profile for the first dose (o) was obtained from injection of a dose of  $^{125}\text{I}$ -HbV administered after hemorrhagic shock. The profile for the second dose (•) was obtained from the injection of a dose of  $^{125}\text{I}$ -HbV 1 hour after injection of the first dose of nonradiolabeled HbV administered after hemorrhagic shock. (B) Determination of IgM against HbV 5 days after a single intravenous injection of HbV to normal rats at a dose of 0.1 mg Hb/kg (closed bars) or 1 hour after a single intravenous injection of HbV to hemorrhagic shock rats at a dose of 1,400 mg Hb/kg (open bars) in mice. IgM against HbV were detected by ELISA. Each bar represents the mean  $\pm$  SD ( $n=3-5$ ).

## Extrapolation to human subjects

From the viewpoint of future clinical applications, predictions of human pharmacokinetics based on data obtained from animal studies—so called, “animal scale-up”—is important for the determination of optimal doses and intervals (Izumi et al., 1996). Thus, we attempted to predict the half-life of HbV in humans using an allometric equation that is generally used in animal scale-up studies. Using the relationships observed for mice (Taguchi et al., 2009b), rats (Taguchi et al., 2009a), and rabbits (Sou et al., 2005), the half-life of HbV in healthy humans was predicted to be approximately 96 hours. In addition, based on half-life data and percent of injected dose values obtained from pharmacokinetic studies of HbV in rats and rabbits, Sou et al. also predicted that the half-life of HbV in healthy humans would be approximately 72 hours (Sou et al., 2005). Further, the half-life of liposomal preparations is empirically 2–3-fold greater in humans than in rats (Gabizon et al., 2003). In fact, the half-life of liposomal doxorubicin (Doxil formulation) in rats and humans is 35 and 56–90 hours, respectively (Gabizon et al., 2003). Therefore, the half-life of HbV in humans would be predicted to be 3–4 days (Sou et al., 2005). For HbV to function as an artificial oxygen carrier, it is desirable that intravascular persistence be at least equal to the time required to regenerate RBCs (Sehgal et al., 1984). Following a massive hemorrhage, the lost blood volume and oxygen-carrying capacity is replaced within approximately 5 days (Hughes et al., 1995; Awasthi et al., 2007). Because the half-life of HbV in humans was estimated to be approximately 3–4 days, HbV would function as a temporary oxygen carrier until a blood transfusion is available or until autologous blood is recovered after a massive hemorrhage.

## Conclusion

Like other drugs, a pharmacokinetic evaluation is an important issue for the development of HbV as a substitute of RBC. In fact, though the perfluorocarbon-based oxygen carriers and acellular-type HBOCs were moved into the clinical trial stages, these artificial oxygen carriers dropped from further clinical development due to severe and unexpected side effects, which might have been predicted from pharmacokinetic analysis data. Therefore, it is also necessary to conduct an in-depth pharmacokinetic study of HbV before moving on to the clinical trial stage.

Our recent preclinical study of HbV clearly demonstrated five major findings on pharmacokinetic profiles. First, HbV and its components have favorable metabolic and excretion profiles in mammalian species, similar to endogenous substances. Second, HbV is safe and useful under conditions of a massive hemorrhage. Third, HbV did not show any toxicity and accumulation in the body, even under conditions of hypometabolism and excretion (i.e., hepatic cirrhosis). Fourth, HbV has the potential to

induce the ABC phenomenon, but the repeated use of HbV at a putative dose would not be expected to induce the ABC phenomenon in a clinical situation. Finally, HbV has a good retention in the blood circulation, and the half-life of HbV in humans was estimated to be approximately 3–4 days, which is sufficient for it to function as an oxygen carrier. These findings support previous views related to the pharmacological efficacy and safety of HbV in normal and hemorrhagic shock model rats from the view point of pharmacokinetics.

In addition to functioning as a substitute for RBCs, HbV would be expected to have a variety of other applications, based on its oxygen transport characteristics, such as in cardiopulmonary bypass priming solutions (Yamazaki et al., 2006), wound healing in critically ischemic skin (Plock et al., 2009), and as a radiation therapy agent (Yamamoto et al., 2009). Therefore, this issue deserves to be studied further, with further data collected in preclinical pharmacokinetic studies for future applications of HbV in the clinic.

## Acknowledgments

The authors acknowledge Emeritus Prof. Eishun Tsuchida, Dr. Hiromi Sakai (Waseda University), Prof. Koichi Kobayashi, Dr. Hirohisa Horinouchi (Keio University), Prof. Shokei Kim-Mitsuyama, Dr. Eiichiro Yamamoto, Dr. Hiroshi Watanabe, Dr. Daisuke Kadowaki, Ms. Yukino Urata, Ms. Mayumi Miyasato (Kumamoto University), Dr. Toshiya Kai (Nipro Corp., Osaka, Japan), Dr. Makoto Anraku (Fukuyama University), Dr. Yasunori Iwao (University of Shizuoka), and their active colleagues for meaningful discussion and contributions to this research.

## Declaration of interest

The authors declare no financial conflicts of interest. The authors alone are responsible for the content and writing of this paper.

## References

- Abe, H., Ikebuchi, K., Hirayama, J., Fujihara, M., Takeoka, S., Sakai, H., et al. (2001). Virus inactivation in hemoglobin solution by heat treatment. *Artif Cells Blood Substit Immobil Biotechnol* 29:381–388.
- Abernethy, D. R., Greenblatt, D. J., Divoll, M., Harmatz, J. S., Shader, R. I. (1981). Alterations in drug distribution and clearance due to obesity. *J Pharmacol Exp Ther* 217:681–685.
- Awasthi, V., Yee, S. H., Jerabek, P., Goins, B., Phillips, W. T. (2007). Cerebral oxygen delivery by liposome-encapsulated hemoglobin: a positron-emission tomographic evaluation in a rat model of hemorrhagic shock. *J Appl Physiol* 103:28–38.
- Balla, J., Vercellotti, G. M., Jeney, V., Yachie, A., Varga, Z., et al. (2005). Heme, heme oxygenase, and ferritin in vascular endothelial cell injury. *Mol Nutr Food Res* 49:1030–1043.
- Bekersky, I., Fielding, R. M., Dressler, D. E., Kline, S., Buell, D. N., Walsh, T. J. (2001). Pharmacokinetics, excretion, and mass balance of <sup>14</sup>C after administration of <sup>14</sup>C-cholesterol-labeled AmBisome to healthy volunteers. *J Clin Pharmacol* 41:963–971.

- Burhop, K., Gordon, D., Estep, T. (2004). Review of hemoglobin-induced myocardial lesions. *Artif Cells Blood Substit Immobil Biotechnol* 32:353-374.
- Chang, T. M., Powanda, D., Yu, W. P. (2003). Analysis of polyethylene-glycol-poly-lactide nano-dimension artificial red blood cells in maintaining systemic hemoglobin levels and prevention of methemoglobin formation. *Artif Cells Blood Substit Immobil Biotechnol* 31:231-247.
- Chen, J. Y., Scerbo, M., Kramer, G. (2009). A review of blood substitutes: examining the history, clinical trial results, and ethics of hemoglobin-based oxygen carriers. *Clinics (Sao Paulo)* 64:803-813.
- Creteur, J., Vincent, J. L. (2003). Hemoglobin solutions. *Crit Care Med* 31:S698-S707.
- Dams, E. T., Laverman, P., Oyen, W. J., Storm, G., Scherphof, G. L., van Der Meer, J. W., et al. (2000). Accelerated blood clearance and altered biodistribution of repeated injections of sterically stabilized liposomes. *J Pharmacol Exp Ther* 292:1071-1079.
- Gabizon, A., Shmeeda, H., Barenholz, Y. (2003). Pharmacokinetics of pegylated liposomal doxorubicin: review of animal and human studies. *Clin Pharmacokinet* 42:419-436.
- Goins, B., Klipper, R., Sanders, J., Cliff, R. O., Rudolph, A. S., Phillips, W. T. (1995). Physiological responses, organ distribution, and circulation kinetics in anesthetized rats after hypovolemic exchange transfusion with technetium-99m-labeled liposome-encapsulated hemoglobin. *Shock* 4:121-130.
- Grone, E. F., Grone, H. J. (2008). Does hyperlipidemia injure the kidney? *Nat Clin Pract Nephrol* 4:424-425.
- Hughes, G. S., Jr., Francome, S. F., Antal, E. J., Adams, W. J., Locker, P. K., Yancey, E. P., et al. (1995). Hematologic effects of a novel hemoglobin-based oxygen carrier in normal male and female subjects. *J Lab Clin Med* 126:444-451.
- Ishida, T., Ichihara, M., Wang, X., Kiwada, H. (2006a). Spleen plays an important role in the induction of accelerated blood clearance of PEGylated liposomes. *J Contr Rel* 115:243-250.
- Ishida, T., Ichihara, M., Wang, X., Yamamoto, K., Kimura, J., Majima, E., et al. (2006b). Injection of PEGylated liposomes in rats elicits PEG-specific IgM, which is responsible for rapid elimination of a second dose of PEGylated liposomes. *J Contr Rel* 112:15-25.
- Ishida, T., Kashima, S., Kiwada, H. (2008). The contribution of phagocytic activity of liver macrophages to the accelerated blood clearance (ABC) phenomenon of PEGylated liposomes in rats. *J Contr Rel* 126:162-165.
- Ishida, T., Maeda, R., Ichihara, M., Irimura, K., Kiwada, H. (2003a). Accelerated clearance of PEGylated liposomes in rats after repeated injections. *J Contr Rel* 88:35-42.
- Ishida, T., Masuda, K., Ichikawa, T., Ichihara, M., Irimura, K., Kiwada, H. (2003b). Accelerated clearance of a second injection of PEGylated liposomes in mice. *Int J Pharm* 255:167-174.
- Izumi, T., Enomoto, S., Hoshiyama, K., Sasahara, K., Shibukawa, A., Nakagawa, T., et al. (1996). Prediction of the human pharmacokinetics of troglitazone, a new and extensively metabolized antidiabetic agent, after oral administration, with an animal scale-up approach. *J Pharmacol Exp Ther* 277:1630-1641.
- Jahr, J. S., Moallempour, M., Lim, J. C. (2008). HBOC-201, hemoglobin glutamer-250 (bovine), Hemopure (Biopure Corporation). *Exp Opin Biol Ther* 8:1425-1433.
- Jahr, J. S., Walker, V., Manoochehri, K. (2007). Blood substitutes as pharmacotherapies in clinical practice. *Curr Opin Anaesthesiol* 20:325-330.
- Kadowaki, D., Anraku, M., Tasaki, Y., Kitamura, K., Wakamatsu, S., Tomita, K., et al. (2007). Effect of olmesartan on oxidative stress in hemodialysis patients. *Hypertens Res* 30:395-402.
- Kiwada, H., Matsuo, H., Harashima, H. (1998). Identification of proteins mediating clearance of liposomes using a liver perfusion system. *Adv Drug Deliv Rev* 32:61-79.
- Kristiansen, M., Graversen, J. H., Jacobsen, C., Sonne, O., Hoffman, H. J., Law, S. K., et al. (2001). Identification of the haemoglobin scavenger receptor. *Nature* 409:198-201.
- Kuipers, F., Spanjer, H. H., Havinga, R., Scherphof, G. L., Vonk, R. J. (1986). Lipoproteins and liposomes as *in vivo* cholesterol vehicles in the rat: preferential use of cholesterol carried by small unilamellar liposomes for the formation of muricholic acids. *Biochim Biophys Acta* 876:559-566.
- Lee, J., Yoon, S., Nho, K. (2006). Pharmacokinetics of 125I-radiolabelled PEG-hemoglobin SB1. *Artif Cells Blood Substit Immobil Biotechnol* 34:277-292.
- Lok, C. (2001). Blood product from cattle wins approval for use in humans. *Nature* 410:855.
- Natanson, C., Kern, S. J., Lurie, P., Banks, S. M., Wolfe, S. M. (2008). Cell-free hemoglobin-based blood substitutes and risk of myocardial infarction and death: a meta-analysis. *JAMA* 299:2304-2312.
- Noble, C. O., Krauze, M. T., Drummond, D. C., Yamashita, Y., Saito, R., Berger, M. S., et al. (2006). Novel nanoliposomal CPT-11 infused by convection-enhanced delivery in intracranial tumors: pharmacology and efficacy. *Cancer Res* 66:2801-2806.
- Nose, Y. (2004). Is there a role for blood substitutes in civilian medicine: a drug for emergency shock cases? *Artif Org* 28:807-812.
- Okamura, Y., Takeoka, S., Eto, K., Maekawa, I., Fujie, T., Maruyama, H., et al. (2009). Development of fibrinogen gamma-chain peptide-coated, adenosine diphosphate-encapsulated liposomes as a synthetic platelet substitute. *J Thromb Haemost* 7:470-477.
- Okumura, H., Katoh, M., Minami, K., Nakajima, M., Yokoi, T. (2007). Change of drug excretory pathway by CCl<sub>4</sub>-induced liver dysfunction in rat. *Biochem Pharmacol* 74:488-495.
- Pape, A., Habler, O. (2007). Alternatives to allogeneic blood transfusions. *Best Pract Res Clin Anaesthesiol* 21:221-239.
- Parry, E. (1988). Blood substitutes: historical perspective. In: Lowe, K. C. (Ed.), *Blood substitute: preparation, physiology, and medical applications* (pp. 17-49). New York: Ellis Horwood.
- Plock, J. A., Rafatmehr, N., Sinovcic, D., Schnider, J., Sakai, H., Tsuchida, E., et al. (2009). Hemoglobin vesicles improve wound healing and tissue survival in critically ischemic skin in mice. *Am J Physiol Heart Circ Physiol* 297:H905-H910.
- Sakai, H., Horinouchi, H., Tomiyama, K., Ikeda, E., Takeoka, S., Kobayashi, K., et al. (2001). Hemoglobin-vesicles as oxygen carriers: influence on phagocytic activity and histopathological changes in reticuloendothelial system. *Am J Pathol* 159:1079-1088.
- Sakai, H., Masada, Y., Horinouchi, H., Ikeda, E., Sou, K., Takeoka, S., et al. (2004a). Physiological capacity of the reticuloendothelial system for the degradation of hemoglobin vesicles (artificial oxygen carriers) after massive intravenous doses by daily repeated infusions for 14 days. *J Pharmacol Exp Ther* 311:874-884.
- Sakai, H., Masada, Y., Horinouchi, H., Yamamoto, M., Ikeda, E., Takeoka, S., et al. (2004b). Hemoglobin-vesicles suspended in recombinant human serum albumin for resuscitation from hemorrhagic shock in anesthetized rats. *Crit Care Med* 32:539-545.
- Sakai, H., Seishi, Y., Obata, Y., Takeoka, S., Horinouchi, H., Tsuchida, E., et al. (2009). Fluid resuscitation with artificial oxygen carriers in hemorrhaged rats: profiles of hemoglobin-vesicle degradation and hematopoiesis for 14 days. *Shock* 31:192-200.
- Sakai, H., Sou, K., Horinouchi, H., Kobayashi, K., Tsuchida, E. (2008). Haemoglobin-vesicles as artificial oxygen carriers: present situation and future visions. *J Intern Med* 263:4-15.
- Sakai, H., Takeoka, S., Yokohama, H., Seino, Y., Nishide, H., Tsuchida, E. (1993). Purification of concentrated hemoglobin using organic solvent and heat treatment. *Prot Expr Purif* 4:563-569.
- Sakai, H., Tomiyama, K. I., Sou, K., Takeoka, S., Tsuchida, E. (2000). Poly(ethylene glycol)-conjugation and deoxygenation enable long-term preservation of hemoglobin-vesicles as oxygen carriers in a liquid state. *Bioconj Chem* 11:425-432.
- Sakai, H., Tsuchida, E. (2007). Hemoglobin-vesicles for a transfusion alternative and targeted oxygen delivery. *J Liposome Res* 17:227-235.
- Savitsky, J. P., Doczi, J., Black, J., Arnold, J. D. (1978). A clinical safety trial of stroma-free hemoglobin. *Clin Pharmacol Ther* 23:73-80.
- Sehgal, L. R., Gould, S. A., Rosen, A. L., Sehgal, H. L., Moss, G. S. (1984). Polymerized pyridoxylated hemoglobin: a red cell substitute with normal oxygen capacity. *Surgery* 95:433-438.



- Shimoishi, K., Anraku, M., Kitamura, K., Tasaki, Y., Taguchi, K., Hashimoto, M., et al. (2007). An oral adsorbent, AST-120, protects against the progression of oxidative stress by reducing the accumulation of indoxyl sulfate in the systemic circulation in renal failure. *Pharm Res* 24:1283-1289.
- Smani, Y. (2008). Hemospan: a hemoglobin-based oxygen carrier for potential use as a blood substitute and for the potential treatment of critical limb ischemia. *Curr Opin Investig Drugs* 9:1009-1019.
- Sou, K., Endo, T., Takeoka, S., Tsuchida, E. (2000). Poly(ethylene glycol)-modification of the phospholipid vesicles by using the spontaneous incorporation of poly(ethylene glycol)-lipid into the vesicles. *Bioconjug Chem* 11:372-379.
- Sou, K., Goins, B., Takeoka, S., Tsuchida, E., Phillips, W. T. (2007). Selective uptake of surface-modified phospholipid vesicles by bone marrow macrophages *in vivo*. *Biomaterials* 28:2655-2666.
- Sou, K., Klipper, R., Goins, B., Tsuchida, E., Phillips, W. T. (2005). Circulation kinetics and organ distribution of Hb-vesicles developed as a red blood cell substitute. *J Pharmacol Exp Ther* 312:702-709.
- Spahn, D. R., Kocian, R. (2003). The place of artificial oxygen carriers in reducing allogeneic blood transfusions and augmenting tissue oxygenation. *Can J Anaesth* 50:S41-S47
- Stowell, C. P. (2005). What happened to blood substitutes? *Transfus Clin Biol* 12:374-379.
- Taguchi, K., Iwao, Y., Watanabe, H., Kadowaki, D., Sakai, H., Kobayashi, K., et al. (2011a). Repeated injection of high doses of hemoglobin encapsulated liposomes (hemoglobin-vesicles) induces accelerated blood clearance in a hemorrhagic shock rat model. *Drug Metab Dispos* 39:484-489.
- Taguchi, K., Maruyama, T., Iwao, Y., Sakai, H., Kobayashi, K., Horinouchi, H., et al. (2009a). Pharmacokinetics of single and repeated injection of hemoglobin-vesicles in hemorrhagic shock rat model. *J Contr Rel* 136:232-239.
- Taguchi, K., Miyasato, M., Ujihira, H., Watanabe, H., Kadowaki, D., Sakai, H., et al. (2010). Hepatically-metabolized and -excreted artificial oxygen carrier, hemoglobin-vesicles, can be safely used under conditions of hepatic impairment. *Toxicol Appl Pharmacol* 248:234-241.
- Taguchi, K., Miyasato, M., Watanabe, H., Sakai, H., Tsuchida, E., Horinouchi, H., et al. (2011b). Alteration in the pharmacokinetics of hemoglobin-vesicles in a rat model of chronic liver cirrhosis is associated with Kupffer cell phagocyte activity. *J Pharm Sci* 100:775-783.
- Taguchi, K., Urata, Y., Anraku, M., Maruyama, T., Watanabe, H., Sakai, H., et al. (2009b). Pharmacokinetic study of enclosed hemoglobin and outer lipid component after the administration of hemoglobin vesicles as an artificial oxygen carrier. *Drug Metab Dispos* 37:1456-1463.
- Taguchi, K., Urata, Y., Anraku, M., Watanabe, H., Kadowaki, D., Sakai, H., et al. (2009c). Hemoglobin vesicles, polyethylene glycol (PEG) ylated liposomes developed as a red blood cell substitute, do not induce the accelerated blood clearance phenomenon in mice. *Drug Metab Dispos* 37:2197-2203.
- Takaori, M. (2005). Approach to clinical trial considering medical ethics and efficacy for HbV, liposome encapsulated hemoglobin vesicle. *Artif Cells Blood Substit Immobil Biotechnol* 33:65-73.
- Terajima, K., Tsueshita, T., Sakamoto, A., Ogawa, R. (2006). Fluid resuscitation with hemoglobin vesicles in a rabbit model of acute hemorrhagic shock. *Shock* 25:184-189.
- Turck, D., Schwarz, A., Hoffer, D., Narjes, H. H., Nehmiz, G., Heinzl, G. (1996). Pharmacokinetics of meloxicam in patients with end-stage renal failure on haemodialysis: a comparison with healthy volunteers. *Eur J Clin Pharmacol* 51:309-313.
- Walsh, T. J., Yeldandi, V., McEvoy, M., Gonzalez, C., Chanock, S., Freifeld, A., et al. (1998). Safety, tolerance, and pharmacokinetics of a small unilamellar liposomal formulation of amphotericin B (AmBisome) in neutropenic patients. *Antimicrob Agents Chemother* 42:2391-2398.
- Wang, X., Ishida, T., Kiwada, H. (2007). Anti-PEG IgM elicited by injection of liposomes is involved in the enhanced blood clearance of a subsequent dose of PEGylated liposomes. *J Contr Rel* 119:236-244.
- Yamamoto, M., Izumi, Y., Horinouchi, H., Teramura, Y., Sakai, H., Kohno, M., et al. (2009). Systemic administration of hemoglobin vesicle elevates tumor tissue oxygen tension and modifies tumor response to irradiation. *J Surg Res* 151:48-54.
- Yamazaki, M., Aeba, R., Yozu, R., Kobayashi, K. (2006). Use of hemoglobin vesicles during cardiopulmonary bypass priming prevents neurocognitive decline in rats. *Circulation* 114:I220-I225
- Zweifach, B. W., Benacerraf, B. (1958). Effect of hemorrhagic shock on the phagocytic function of Kupffer cells. *Circ Res* 6:83-87.

# Determination of electrolyte concentrations in serum containing cellular artificial oxygen carrier (HbV)

Seiji Miyake <sup>(1)</sup>, Jiro Takemura <sup>(1)</sup>, Masuhiko Takaori <sup>(2)</sup>

## Abstract

We attempted to measure electrolyte (Na, K, C) ion concentrations in serum containing an artificial oxygen carrier, HbV (hemoglobin encapsulated liposome vesicle emulsified in physiological saline), by dry chemical method using Vitros250™ (Ortho Clinical Diagnostics) or conventional wet method using TBA200FRNEO™ (Toshiba Medical System). Clinically satisfactory values of the electrolyte ion concentrations were obtained in the serum which contained the HbV at 1/2 ~ 1/32 volume ratio and even in original HbV emulsion by the dry chemistry method. By the wet method, however, satisfactory values with clinically acceptable accuracy were not obtained when mixing volume rate of the HbV remained above 1/8 mixing rate. Subsequently the satisfactory values were obtained when mixing rate of the HbV in serum reduced less than 1/16. Reason for the above limited capacity for the wet method remained obscure. Further a trace amount of potassium ion in the HbV emulsion was a puzzle.

## Keywords

cellular artificial oxygen carrier, serum electrolyte determination, dry chemistry, liposome encapsulated hemoglobin, polarographic examination

## 1. Introduction

It has been desired to develop a therapeutic agent which can restore the circulating blood volume and also oxygen carrying capacity of blood for treatment of massive hemorrhage instead of transfusion of blood, which should be stored at  $5 \pm 1$  °C and compatibility test must be required. Such therapeutic agent is expected most useful for initial treatment e.g. in accident field by Medicares and most effective for life saving for out-of-hospital patient care. Up date, two types of candidate, namely hemoglobin based oxygen carrier (HBOC) and perfluorocarbon based oxygen carrier, were tested for this purpose. Unfortunately development for the latter was discontinued due to short life span in the circulation and also to thrombocytopenia after infusion<sup>1)</sup>. On the other hand for the former, acellular type, it has been pointed out arteriolar vasoconstriction due to its scavenging effect of nitric oxide from endothelial cells<sup>2,3,4)</sup> and consequent coronary events<sup>5)</sup> after its infusion. Thus two pharmaceutical companies have withdrawn from the HBOC

development in early 2009. Only liposome encapsulated hemoglobin vesicle which is emulsified in the physiological saline (HbV) remains to be developed further as HBOC without noticeable adverse effects.

In general, however, it has been reported that HBOCs could interfere clinical laboratory tests<sup>6,7,8)</sup>, particularly spectrophotometry used that would be interfered by absorbancy of hemoglobin molecule. Moreover laboratory test without spectrophotometry, such as polarographic examination, would be suspected to be interfered by the HbV. Since the HbV vesicles covered with non-electroconductive phospholipid, their adherence on electrode surface might effect on boundary potential.

This study was carried out to demonstrate whether or not analyzers commonly used in practice could work well for measurement of electrolyte concentrations in serum containing a cellular artificial oxygen carrier, HbV.

(1) Osaka Prefecture Saiseikai Noe Hospital

(2) East Takarazuka Sato Hospital, 2-1 Nagao-cho Takarazuka-city Hyogo 665-0873, JAPAN

論文受付 2009年12月15日 論文受理 2010年1月18日

## 2. Materials and Methods

Experimental procedures were performed in Osaka Prefecture Saiseikai Noe Hospital. Blood of 18 ml was donated by six healthy, adult volunteers for each who had consented to an informed consent which had stated purpose and procedure of the study and which had been authorized by ethics committee of the hospital. The experimental procedures were examined and regulated by the ethics committee. The HbV was produced and supplied by Nippro Co (Kusatsu, Shiga), which is one of member in research group of Japanese Ministry of Health, Welfare and Labor Research Project "Clinical Applications of Artificial Oxygen Carrier H18-Drug Innovation H18-General-022". Physicochemical properties for the HbV was listed in Table 1. Medium of the HbV was collected by ultracentrifugation (50,000 G for 30 minutes) and supplied by Dr. Sakai, H., Associate Professor, Waseda University who is also one of member in the above research project.

Table 1. Physicochemical properties of HbV

diameter of vesicle ( nm ) .....	270
vesicle volume ( HbVcrit % ) .....	> 30
hemoglobin content ( g/dL ) .....	9.7
phospholipid content ( g/dL ) .....	6.7
hemoglobin / phospholipid ratio .....	1.5
carbon monoxide hemoglobin ( % ) .....	0.1
endotoxin ( EU/ml ) .....	< 0.3
sterility test .....	passed

Blood of 2 ml was collected in EDTA-2K tube and used to determine hematocrit and hemoglobin value. Serum of approximately 9 ml was collected in a serum separating vacuum tube by centrifugation with 1,300 G for 30 minutes from remained blood. Human albumin powder (A3782-1G Sigma-Aldrich, St Louis, Mo, U.S.A.) was dissolved at 4 % in the HbV and the medium separated from HbV.

The HbV was mixed with the original serum at 1:1 volume ratio (1/2 mixture of the HbV). Subsequently a part of this mixture was mixed with the original serum at 1:1

volume ratio and 1/4 mixture of the HbV was prepared. Then serial mixtures, 1/8 ~ 1/32, were prepared in the same manner. Electrolyte concentrations (Na<sup>+</sup>, K<sup>+</sup>, Cl<sup>-</sup>) were measured duplicated for the original serum, serial mixtures of HbV and serum, HbV and medium of HbV with dry (D) method<sup>※</sup> mounted on Vitros250<sup>™</sup> (Ortho Clinical Diagnostics, Rochester, N.Y., U.S.A) and wet (W) method<sup>※</sup> mounted on TBA200FRNEO<sup>™</sup> (Toshiba Medical System, Ohtawara, Tochigi), respectively. The above experimental procedure was repeated on five other days. Consequently total 12 measurements were performed for each same categorized sample with the both methods, respectively. Concentration of the electrolytes in the mixtures of HbV and serum was estimated by simple, mathematical dilution equation. For example, Na<sup>+</sup> concentration in the 1/2 mixture was calculated as follows

$$\text{Na (1/2 mixture)} = (1/2 A + 1/2 \times 0.7 \times 154) \div (1/2 + 1/2 \times 0.7)$$

where A is concentration of Na<sup>+</sup> in the original serum and 0.7 is ratio of water volume contained in aliquot volume of the HbV. Since liposome encapsulated hemoglobin vesicles were emulsified in the physiological saline at volume of 30 % , Na<sup>+</sup> concentration for the medium of HbV was adapted to Na<sup>+</sup> concentration of the physiological saline of 154 mEq/L. Mean and standard deviations for actually measured value (Am ± SD), estimated value (Em ± SD) calculated the above equation and difference (Dm ± SD) between the actually measured value and the estimated value were provided for each measurement.

When the Dm was less than 20 mEq/L for Na<sup>+</sup>, less than 0.05 mEq/L for K<sup>+</sup> and less than 20 mEq/L for Cl<sup>-</sup>, actually measured value corresponded to those Dms for each was evaluated as acceptably determined value, respectively.

Hematocrit and hemoglobin value for the original blood was measured with RBC pulse height detection method and sodium lauryl sulfate hemoglobin method, respectively, using Automated Hematology Analyzer XE-2100<sup>™</sup> (Sysmex Corp. Kobe, Hyogo).

※ When we measure concentration of electrolytes in sample (serum of plasma) using the dry method which is mounted of Vectors250<sup>™</sup> (Ortho Clinical Diagnostics), we inject the sample and reference solution into a small cylinder with maximum capacity of 500μl for each and put those cylinders on each proper position inside of the analyzer. The analyzer sucks up the sample and reference solution with a needle simultaneously and drops them at each proper spot on a piece of film which specific electrode for Na, K, and Cl ion are built in, respectively. After measurement we take out the film and the cylinders and discard them. Therefore any fluid remains inside of the analyzer and so we call the above procedure as dry method.

On the other hand for the wet method, each specific electrode adapted to the ions is provided in capillary part inside of an analyzer, for example, TBA200FRNEO<sup>™</sup> (Toshiba Medical System). The capillary is always filled with special reference solution for the ions and calibrated. Therefore we call it as wet method.

Table 2. Electrolyte concentrations for the original serum (serum), serial mixtures of the original HbV and the serum, and the original HbV (HbV)

		HbV	HbV in the mixtures					serum	
			1/2	1/4	1/8	1/16	1/32		
Na <sup>+</sup>	D	Am	155.0±2.2	148.0±1.9	147.1±2.2	146.4±2.4	145.8±2.6	145.3±2.8	143.0±2.5
		Em		148.1±1.5	145.9±2.1	146.4±2.3	144.3±2.5	144.2±2.5	
		Dm		0.0±0.9	1.2±0.5	0.0±0.5	1.5±0.9	1.2±0.7	
	W	Am	110.2±1.4	125.7±1.0	134.6±1.3	138.7±1.5	140.8±1.7	141.8±1.6	142.0±1.3
		Em		147.0±0.8	144.5±1.0	144.8±1.2	142.7±1.2	142.4±1.3	
		Dm		-21.3±0.9	-9.9±1.0	-6.1±0.9	-1.8±1.0	-0.5±0.8	
K <sup>+</sup>	D	Am	ND	2.22±0.18	3.12±0.22	3.53±0.25	3.71±0.25	3.82±0.25	3.93±0.30
		Em		2.32±0.18	3.20±0.30	3.61±0.29	3.77±0.30	3.86±0.31	
		Dm		-0.10±0.06	-0.05±0.07	-0.07±0.07	-0.05±0.08	-0.05±0.08	
	W	Am	0.35±0.01	1.94±0.13	2.89±0.17	3.36±0.18	3.60±0.20	3.72±0.20	3.85±0.25
		Em		2.27±0.16	3.11±0.20	3.54±0.24	3.70±0.25	3.78±0.26	
		Dm		-0.33±0.07	-0.22±0.07	-0.18±0.08	-0.10±0.07	-0.05±0.08	
Cl <sup>-</sup>	D	Am	150.0±6.7	126.7±3.5	115.9±2.4	111.1±2.3	109.4±2.5	108.4±2.1	107.0±1.7
		Em		126.5±1.0	116.2±1.4	112.7±1.7	109.1±1.8	108.1±1.8	
		Dm		0.2±2.7	-0.3±1.3	-1.6±0.8	0.4±1.2	0.3±1.0	
	W	Am	105.3±1.21	104.5±0.9	104.8±1.1	104.8±1.3	104.9±1.6	104.8±1.5	103.9±1.7
		Em		124.6±1.1	113.6±1.4	109.7±1.6	106.0±1.7	104.9±1.7	
		Dm		-20.1±0.4	-8.8±0.5	-4.9±0.5	-1.1±0.7	-0.2±0.6	

D : dry method      W : wet method

serum = the original serum obtained from the volunteers

n = 12    mean ± standard deviations    ND : not detectable

Am : mean for actually measured values      Em : mean for estimated values by the mixing equation (\* see text)

Dm : mean for differences between Am and Em corresponded

mEq/L

### 3. Results

As shown on upper column in Table 2, Na<sup>+</sup> concentration was determined as 155.0±2.2 mEq/L for the original HbV and 143.0±2.5 mEq/L for the original serum with the D method. Difference (Dm) between actually measured 148.0±1.9 mEq/L for the 1/2 mixture and 148.1±1.5 mEq/L for its estimated value was 0.0±0.9 mEq/L. Subsequently Dms with the D method measurement were distributed in a range of 0.0±0.5 ~ 1.5±0.9 mEq/L for the 1/4 ~ 1/32 mixtures.

On the other hand with the W method, Na<sup>+</sup> concentration for HbV and 1/2 mixture were measured as 110.2±1.0 mEq/L and 125.7±1.0 mEq/L with Dm of -21.3±0.9 mEq/L, respectively. Subsequent Dm for the 1/4 and 1/8 mixture were -9.9±1.0 and -6.1±0.9 mEq/L, respectively and therefore those Ams were not evaluated as the acceptably determined value. Dm with Na<sup>+</sup> concentration for the 1/16 and 1/32 mixture, however, was 1.8±1.0 and 0.5±0.8 mEq/L, respectively. Those were less than 2.0 mEq/L and

those actually measured values were evaluated as the acceptably determined value.

K<sup>+</sup> concentrations were listed on middle column in Table 2. K<sup>+</sup> concentration for the HbV could not be measured by the D method. Since the analyzer the D method mounted showed "ND" (not detectable) on its display panel. However subsequent actually measured values of K<sup>+</sup> concentration for the 1/2 ~ 1/32 mixture distributed in a range of 3.12 ~ 3.82 mEq/L and Dms were less than -1.00±0.06 mEq/L with the D method.

With the W method, on the other hand, K<sup>+</sup> concentration for the HbV was determined as 0.35±0.01 mEq/L and Dms for the serial mixtures of 1/2 ~ 1/32 distributed in a range of -0.33±0.07 ~ -0.05±0.08 mEq/L. Those Dms became smaller corresponded to decreasing in the mixing rate of the HbV down to the 1/32 mixture.

As shown on lower column, Cl<sup>-</sup> concentration measured with the D method was 126.7±3.5 mEq/L with Dm of 0.2±